

5. Inverter-fed induction machines



Source: ELIN EBG Motoren GmbH, Austria

5. Inverter-fed induction machines

5.1 Basic performance of variable-speed induction machines

5.2 Drive characteristics of inverter-fed standard induction motors

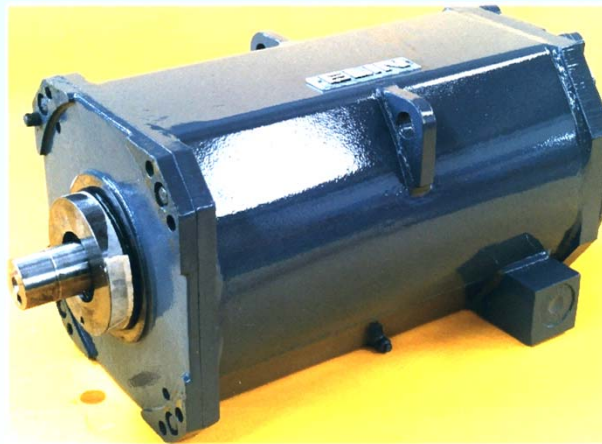
5.3 Features of special induction motors for inverter operation

5.4 Influence of inverter harmonics on motor performance



5. Inverter-fed induction machines

5.1 Basic performance of variable-speed induction machines



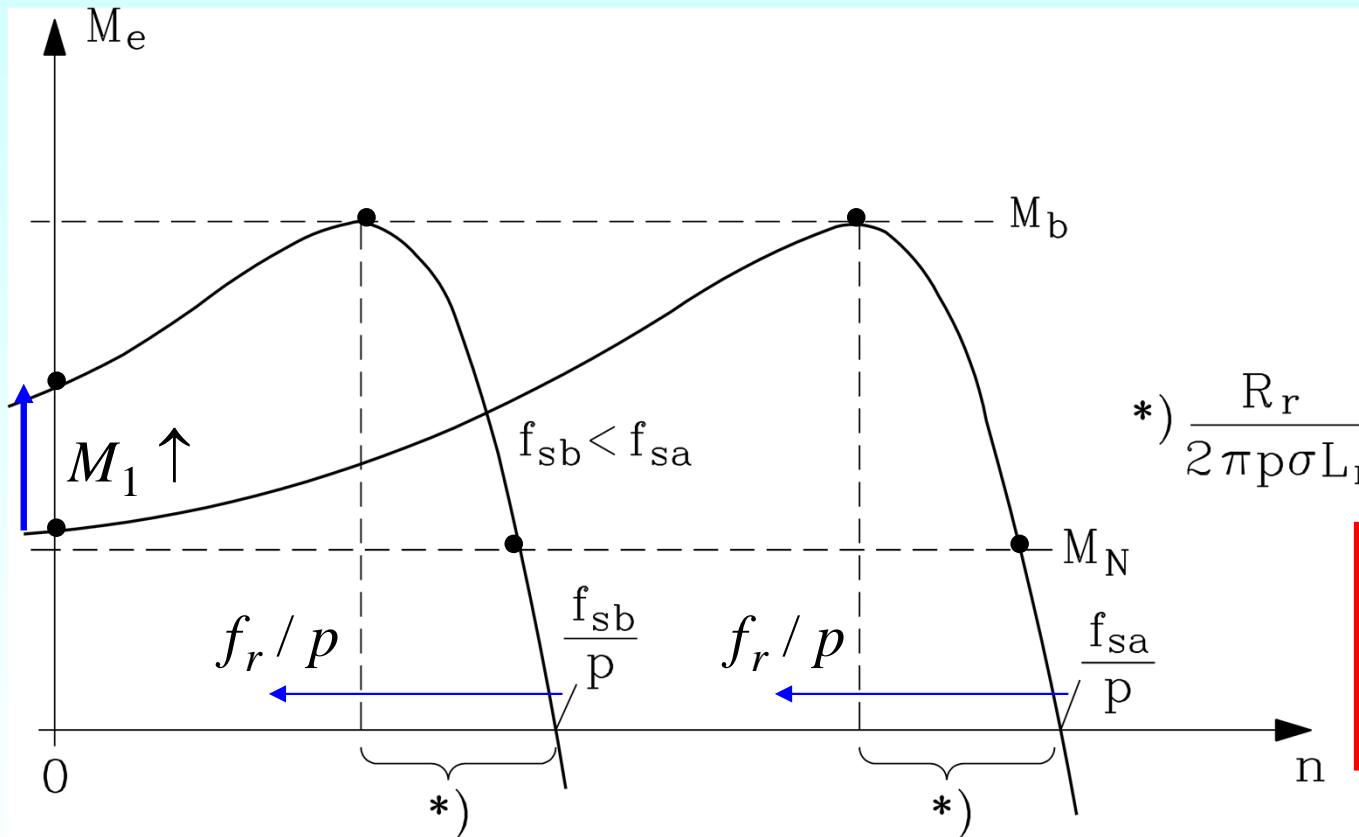
Source: ELIN EBG Motoren GmbH, Austria

Stator winding air gap flux density distribution

Voltage-source inverters with DC voltage link:

$$400 \text{ V grid, } U_d = (3/\pi) \cdot \sqrt{2} \cdot 400 = \underline{\underline{540 \text{ V}}}$$

With neglected stator resistance (*Kloss* function) break down torque is independent of frequency, if voltage fundamental varies linear with frequency:



$$*) \frac{R_r}{2\pi p \sigma L_r} = \frac{f_b}{p} \quad \boxed{U_s \sim f_s} \quad f_r = s \cdot f_s$$

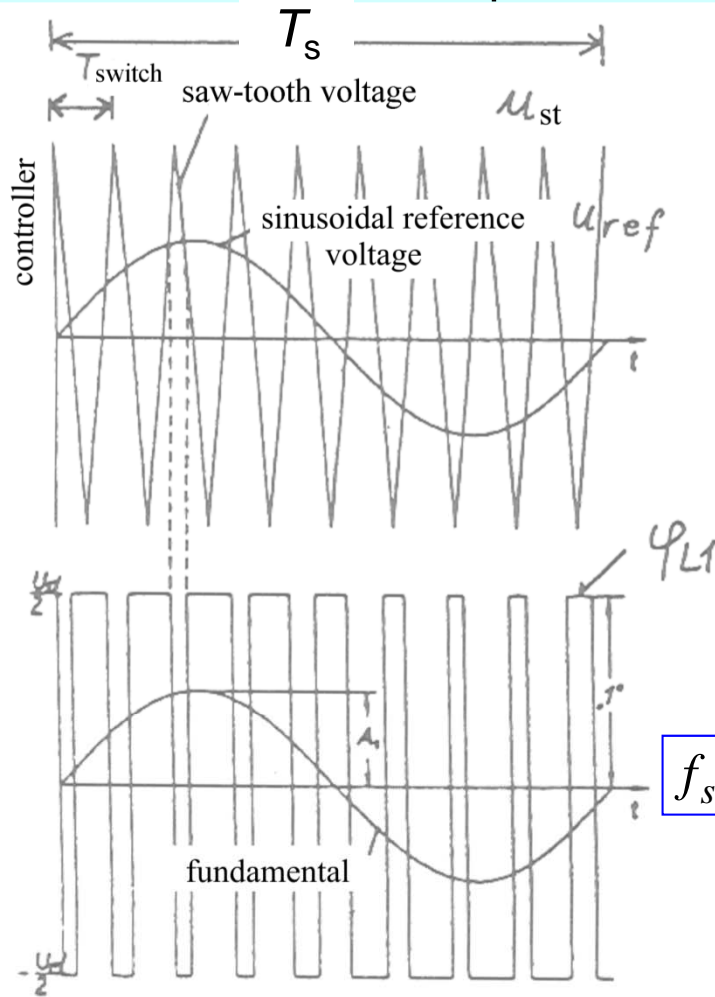
$$R_s = 0: \quad \frac{M_e}{M_b} = \frac{2}{\frac{s_b}{s} + \frac{s}{s_b}} = \frac{2}{\frac{\omega_b}{\omega_r} + \frac{\omega_r}{\omega_b}}$$

$$R_s = 0: \quad M_b = \pm \frac{m_s}{2} \frac{p}{\omega_s} U_s^2 \frac{1-\sigma}{\sigma X_s} = \pm \frac{m_s}{2} \frac{p}{2} \Psi_s^2 \frac{1-\sigma}{\sigma L_s} \quad \frac{U_s}{\omega_s} = \frac{\Psi_s}{\sqrt{2}} \quad \frac{s_b}{s} = \frac{s_b f_s}{s f_s} = \frac{\omega_b}{\omega_r} = \frac{f_b}{f_r}$$

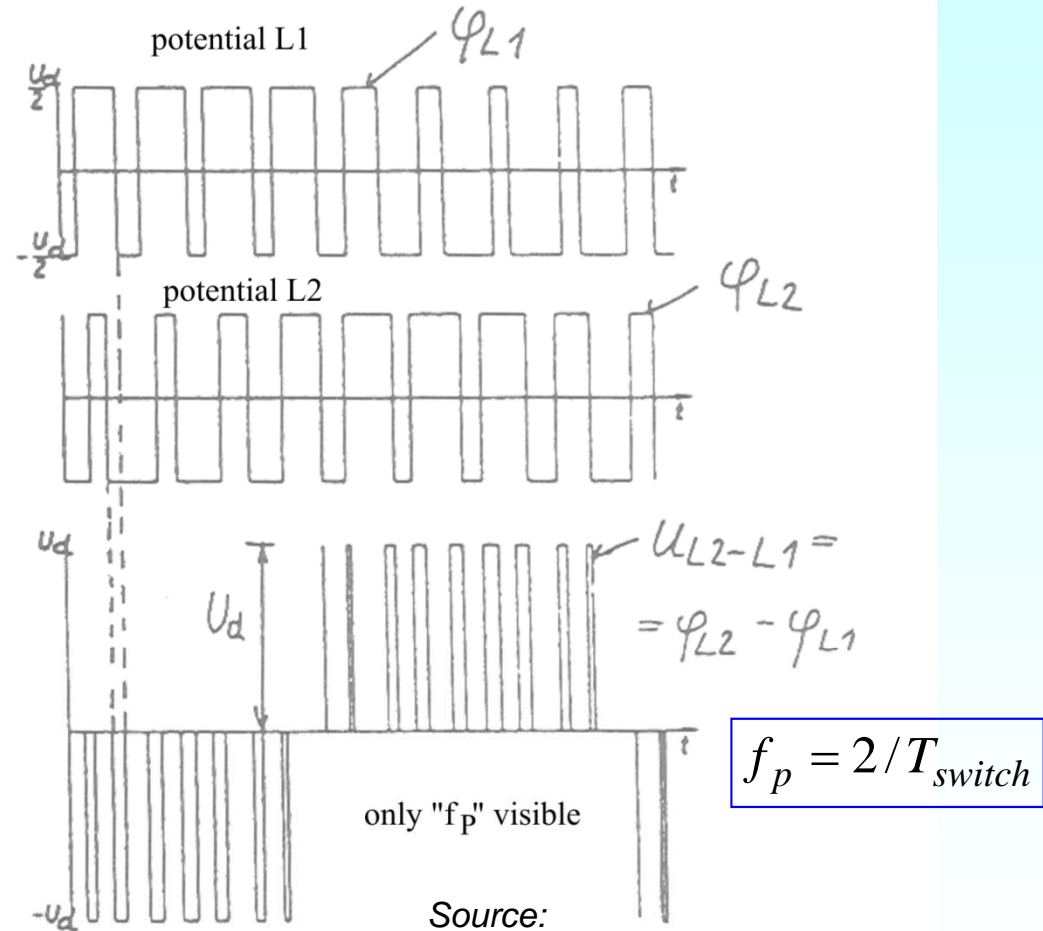


Generation of PWM voltage

- a) Comparison of **saw tooth and reference signal** lead to PWM control signal for power switches: Potential $\varphi_{L1}(t)$ at terminal L1 varies with that PWM signal
- b) Difference of two terminal potentials delivers **line-to-line voltage** $u_{L1-L2}(t)$



a)



b)

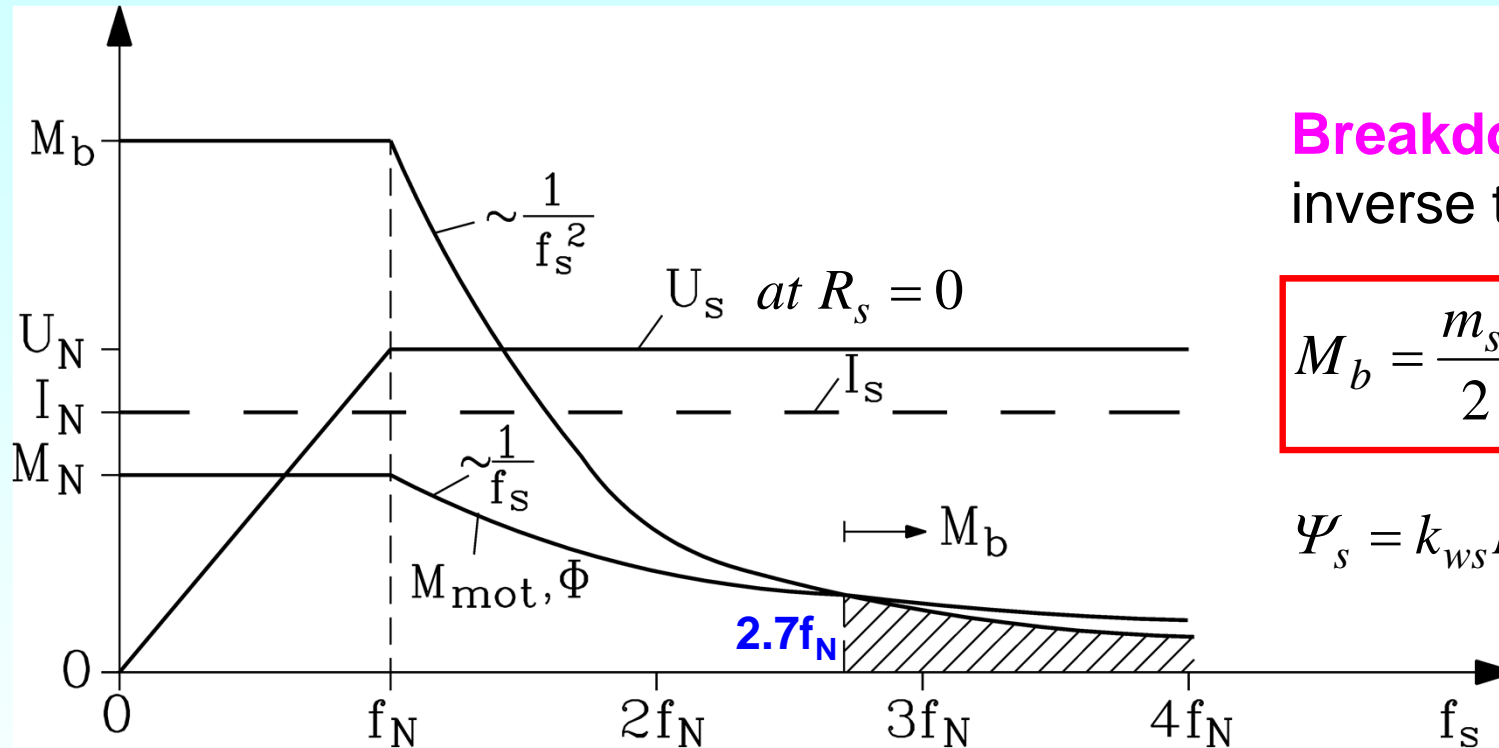
Source:

Kleinrath. H.; Springer, 1980



Constant power range

Voltage stays constant: Power $\sim U \cdot I = \text{const}$; torque decreases inverse to frequency: $M_{eN} = P_N \cdot p / (\omega_s - \omega_{r,N}) \rightarrow M_e \approx M_{mot} = P_N \cdot p / \omega_s \Leftrightarrow M_e \sim I_s \Psi_s \sim I_s U_s / \omega_s$



Breakdown torque decreases inverse to square of frequency:

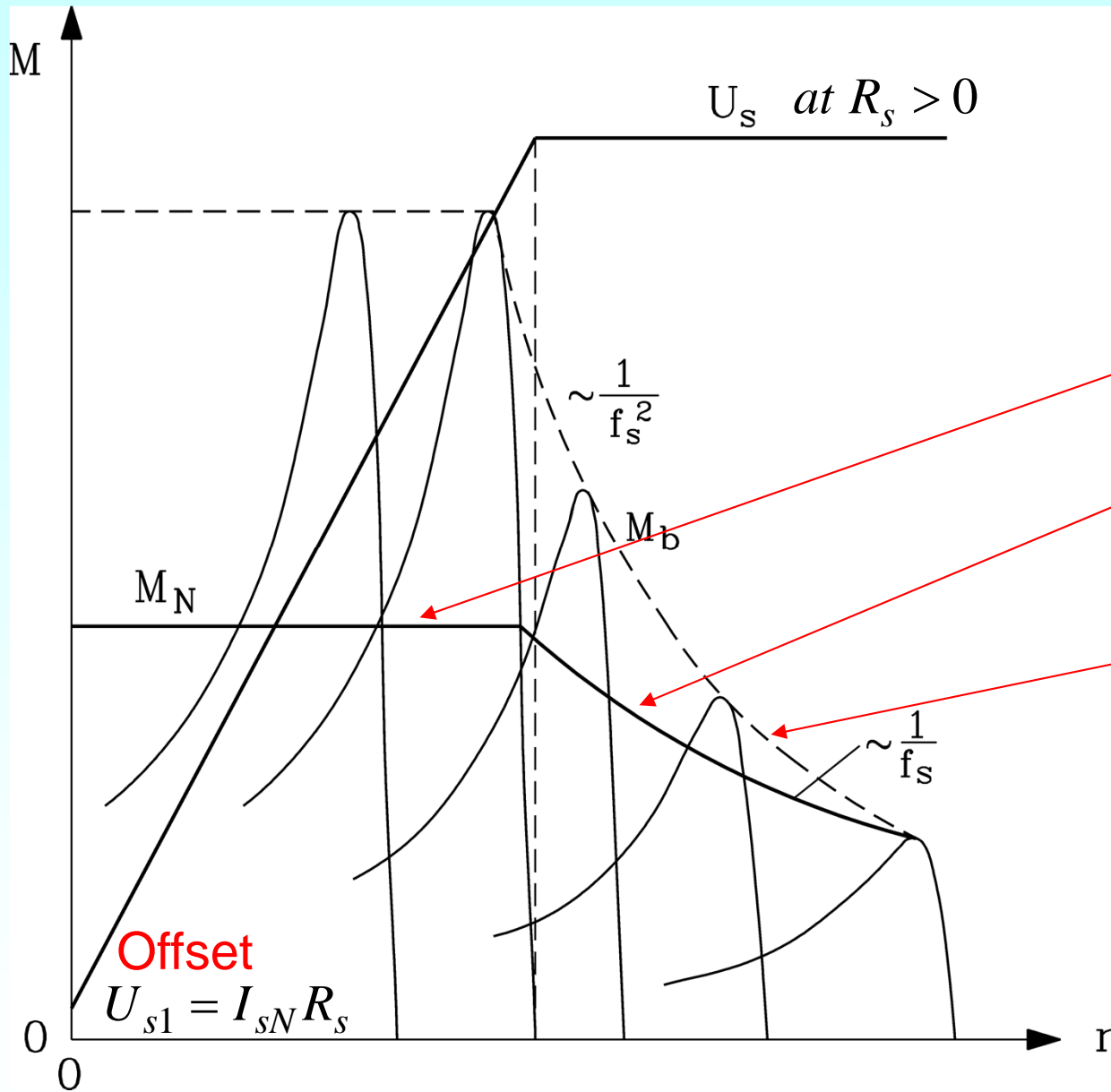
$$M_b = \frac{m_s}{2} \frac{p}{\omega_s} U_{s,\max}^2 \frac{1-\sigma}{\sigma \omega_s L_s} \sim 1/\omega_s^2$$

$$\Psi_s = k_{ws} N_s \Phi$$

Constant rated power range is limited, where decreasing breakdown torque reaches torque demand for rated power: e.g. $2.7f_N$.

Usually maximum frequency $f_{s,\max}$ is defined, where $M_b/M_N = 1.6$ (60% overload margin).

Variable speed torque-speed curves with voltage limit



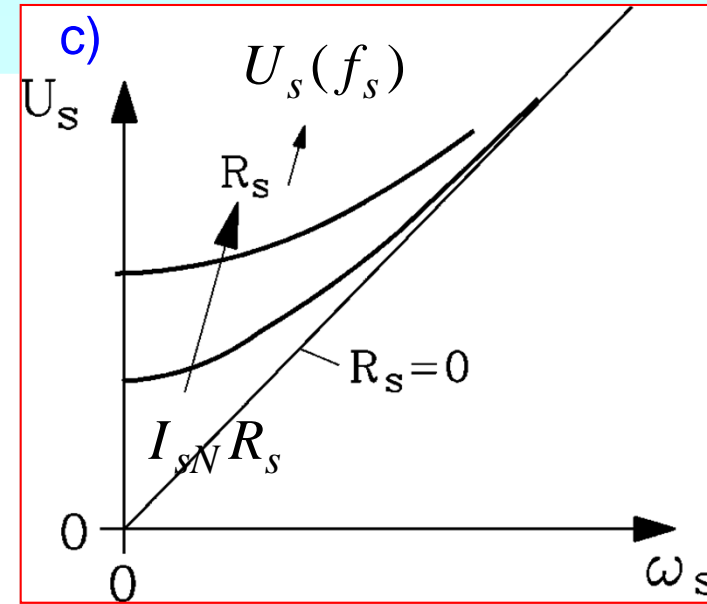
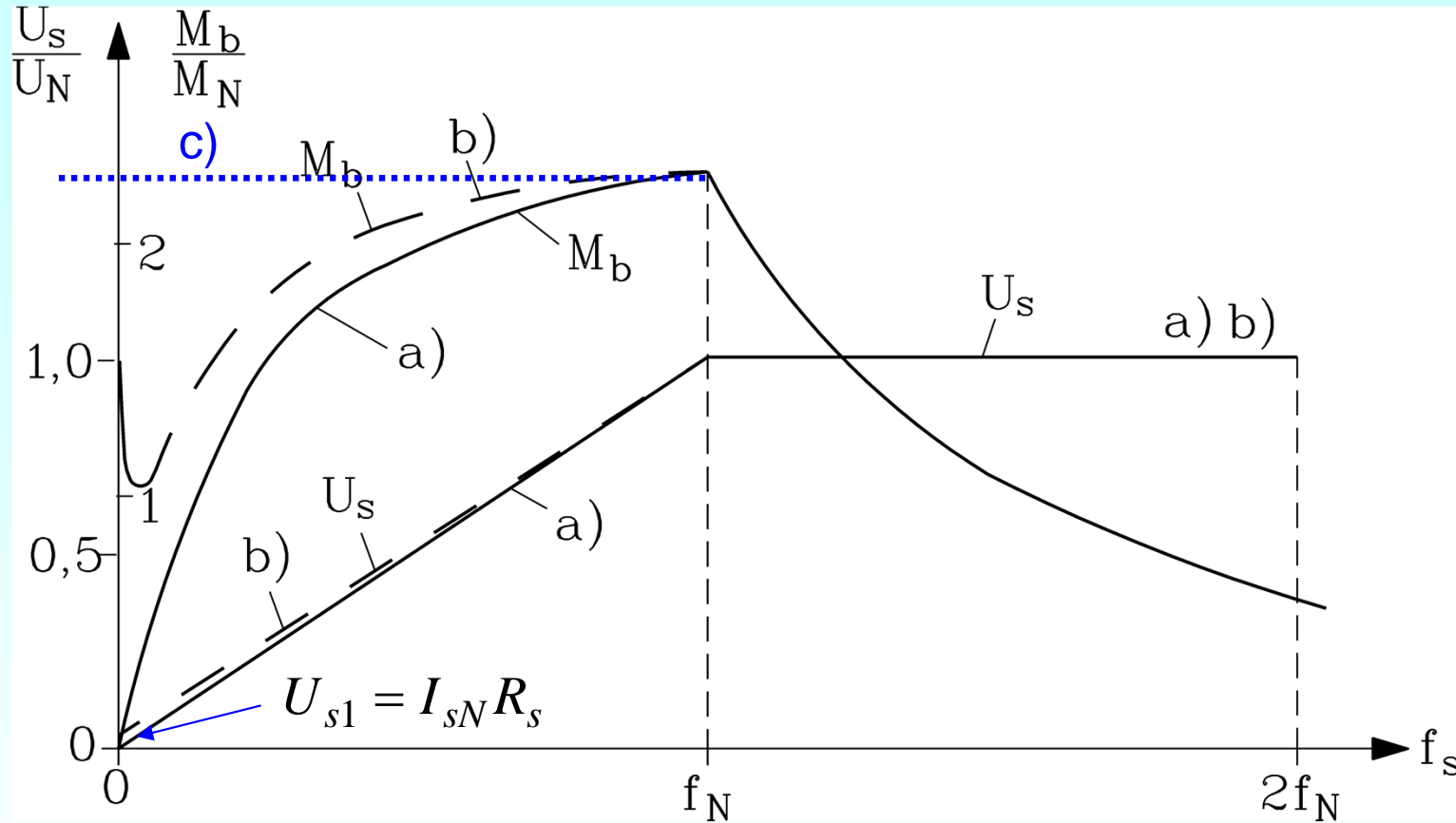
Constant torque

Constant power

Voltage limit



Variable speed induction motor at $R_s > 0$



$$0 \leq f_s \leq f_N :$$

$$a) U_s \sim f_s$$

$$b) U_s = (U_N - U_{s1}) \cdot \frac{f_s}{f_N} + U_{s1}$$

$$c) U_s(f_s)$$

a) Linear rise of voltage with frequency $U_s \sim f_s$:

Breakdown torque decreases with decreasing speed

b) **Additional voltage offset** $U_{s1} = R_s I_s$ at zero speed to compensate resistive voltage drop: Breakdown torque stays above rated torque

5. Inverter-fed induction machines

5.2 Drive characteristics of inverter-fed standard induction motors



Source:
Siemens AG

Loss variation in inverter-fed standard induction motors

- **Cooling air flow** of shaft-mounted fan rises linear with speed: $\dot{V} \sim n / n_N \sim f_s / f_N$

- **Iron losses** in stator: rise with square of flux, with frequency exponent $x \cong 1.8$:

$$P_{Fe} \sim (\Psi / \Psi_N)^2 \cdot (f_s / f_N)^x \quad \text{Hysteresis} \sim f, \text{ eddy currents} \sim f^2$$

- **Friction losses** (bearings $\sim n \dots n^2$), **windage losses** (fan $\sim n^3$): exponent $y = 2,5 \dots 3$:

$$P_{fr+w} \sim (n / n_N)^y \sim (f_s / f_N)^y$$

- **Stray load losses** (caused by space harmonic effects): $z \cong 1.5 \dots 2$

$$P_{ad1} \sim (n / n_N)^z \cdot (I_s / I_N)^2$$

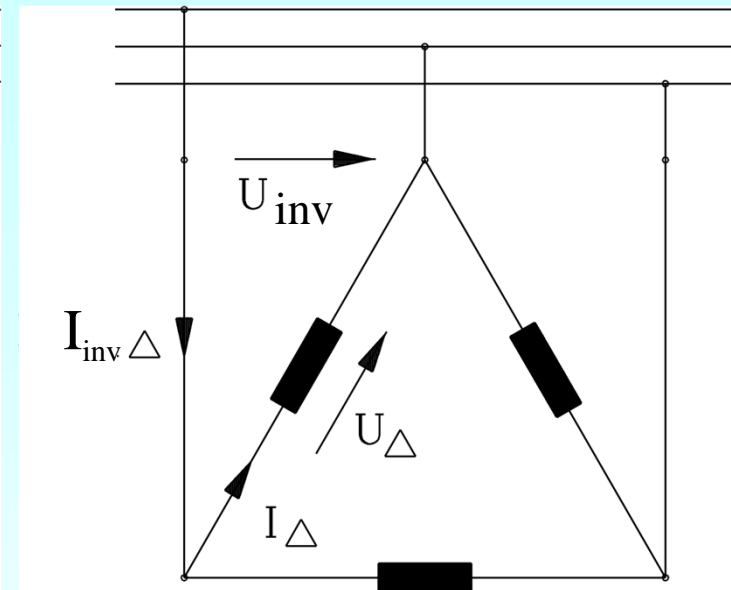
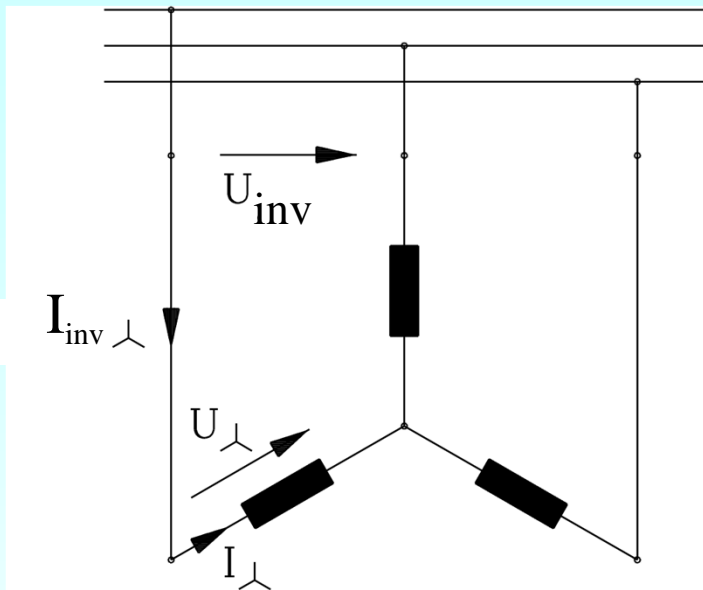
- tooth flux pulsations
- harmonic rotor currents I_{rv}
- harmonic inter-bar currents I_{qv}

Variable air flow in inverter-fed standard induction motors with shaft-mounted fan

- $f_s > f_N$: **Flux weakening:** $\Psi \sim 1/f_s$:
Iron & copper losses constant;
frequency limit: breakdown/rated power reaches 160%.
- $f_{th} < f_s < f_N$: **Constant torque range:**
Iron losses and air flow decrease: at f_{th} , e.g. $f_{th} \sim 0.5f_N$ thermal limit.
- $f_s < f_{th}$: **Reduced torque operation:**
Reduction of current to decrease copper losses due to low air flow



Y-D (star-delta) to increase power by speed



$$U_s \sim f_s$$

- **Star:** Phase voltage $U_Y = U_{inv} / \sqrt{3}$, phase current $I_Y =$ inverter current $I_{inv,Y}$.
- **Delta:** Phase voltage $U_{\Delta} =$ Line-to-line voltage U_{inv} , Phase current $I_{\Delta} = I_{inv,\Delta} / \sqrt{3}$

$$U_Y \sqrt{3} = U_{\Delta} \quad f_{s\Delta} = \sqrt{3} f_{sY} \text{ for same flux} \Rightarrow \text{Inverter current: } I_Y \sqrt{3} = I_{\Delta}$$

Increase of phase voltage in “delta” by 73% allows increase of speed by 73% from 50 Hz to 87 Hz for constant torque. So power increases by 73%, but also current !

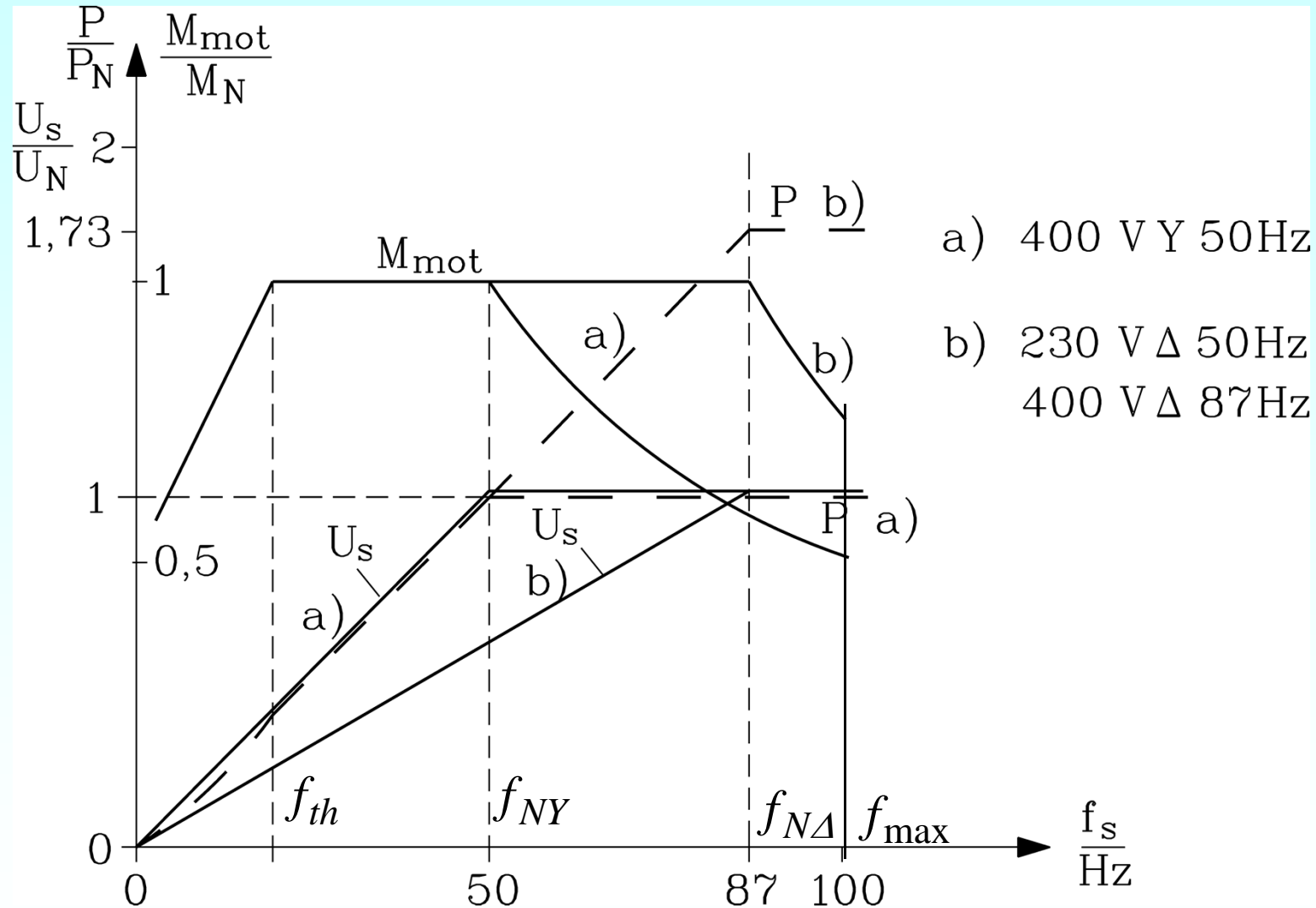
Motor power increase with delta connection

Example: 4-pole induction motor, power factor 0.85, efficiency 90%

stator winding connection	<i>star</i>	<i>delta</i>
inverter maximum output voltage line-to-line $U_{LL,max}$	400 V	400 V
motor maximum phase voltage $U_{s,max}$	230 V	400 V
motor frequency $f_s = f_N$ at $U_{s,max}$	50 Hz	87 Hz
motor rated phase current I_{sN}	100 A	100 A
motor rated line current I_{sN}	100 A	173 A
Motor rated torque M_N	336 Nm	336 Nm
motor output power $P = 2\pi f_N M_N / p$	52.3 kW	90.6 kW
inverter power rating $S = \sqrt{3} U_{LL,max} I_{sN}$	69 kVA	119.4 kVA

Increase of constant torque range & output power

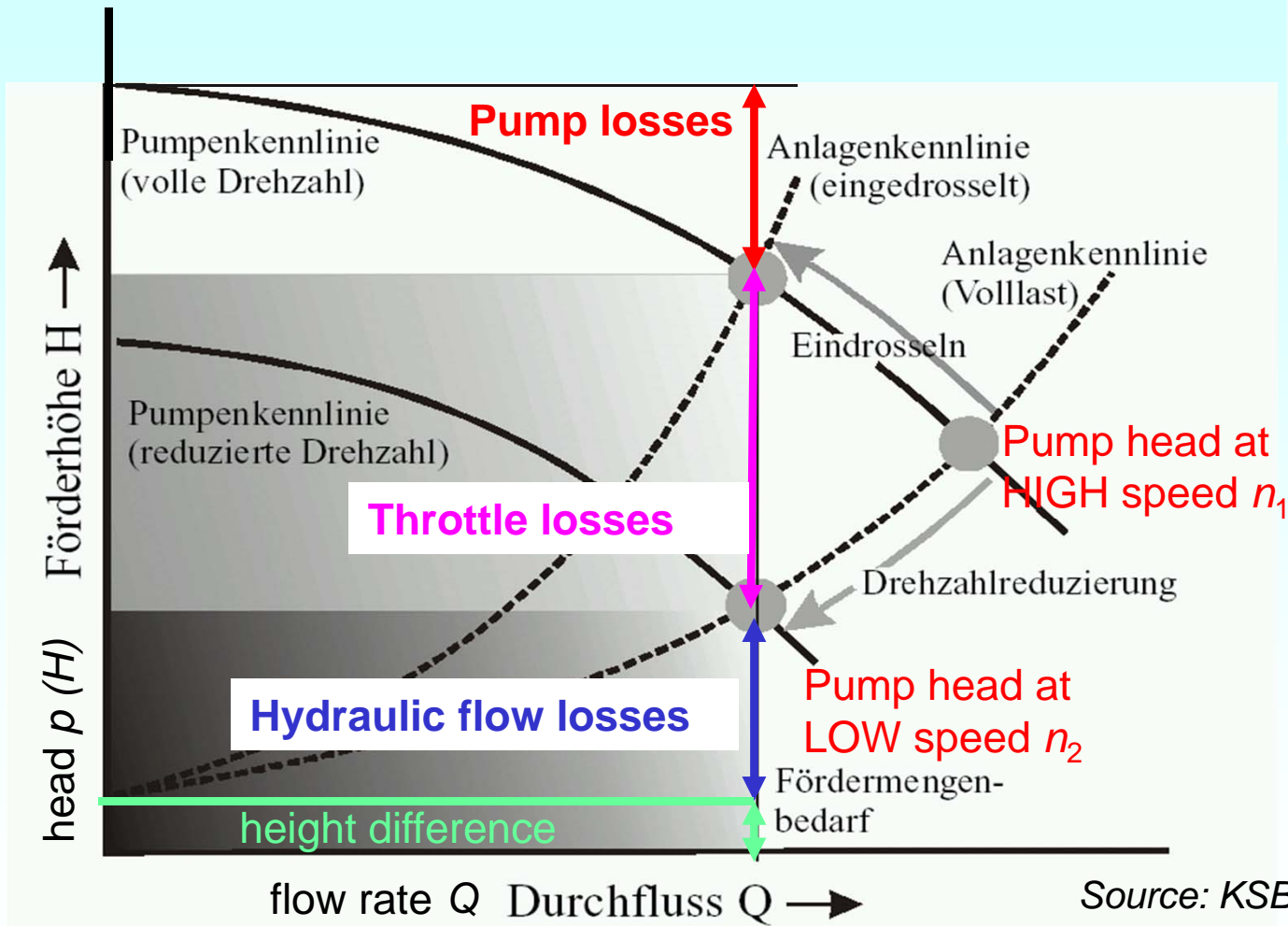
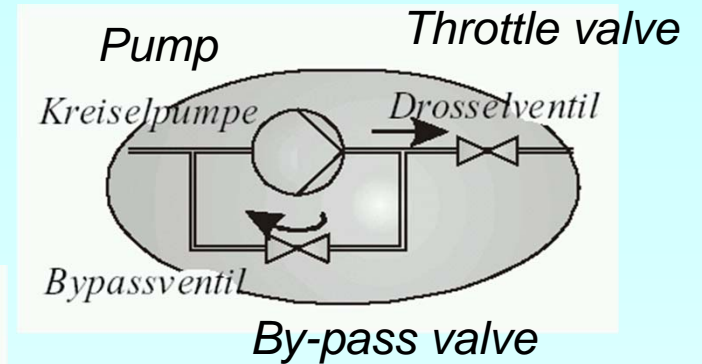
By switching the winding from a) star to b) delta connection !



Application: Variable speed drive for pumping

Example:

The flow rate Q shall be changed!

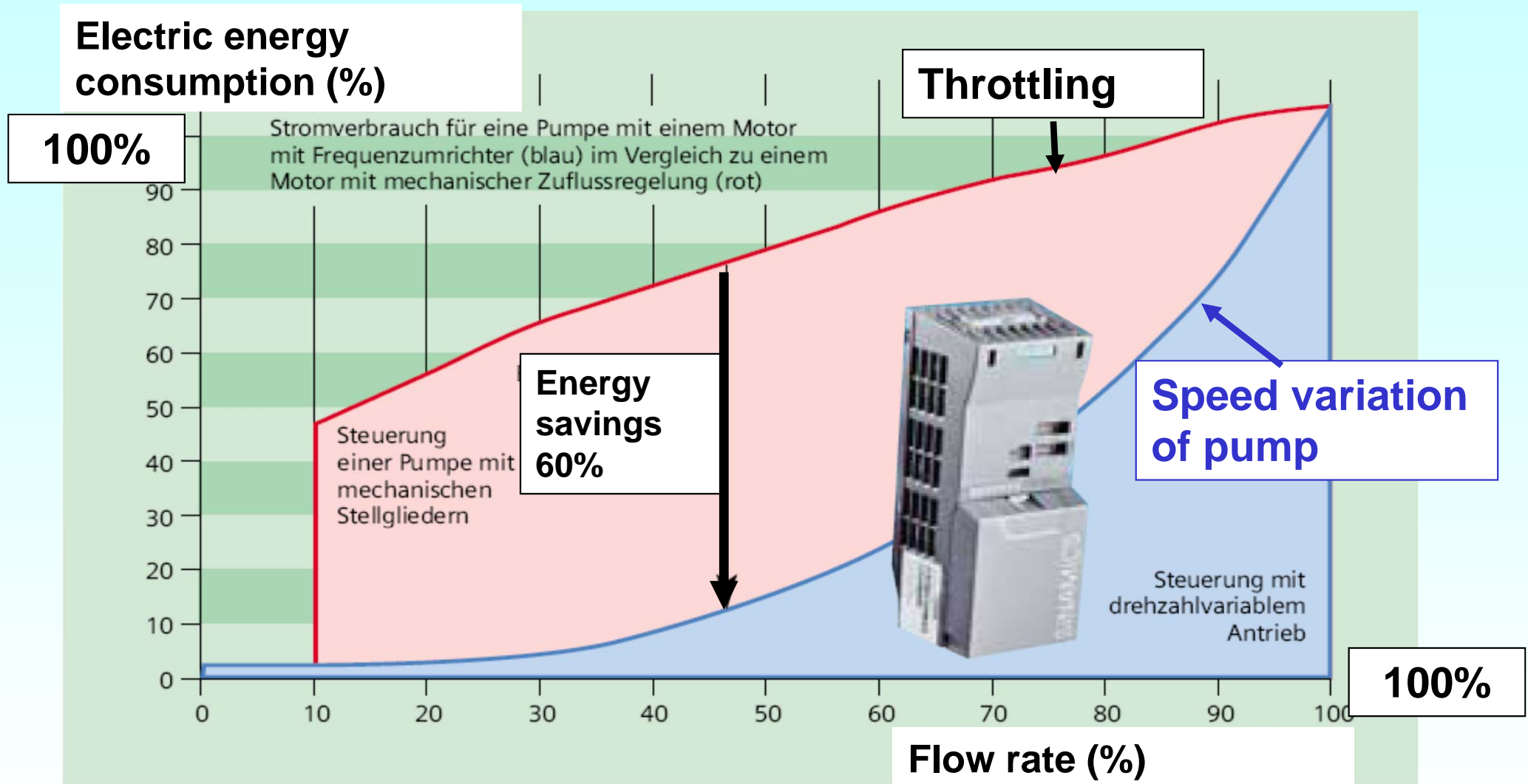


Flow rate variation

a) by throttling: Pump operates at fixed speed

b) by speed variation: Lower pump speed = lower flow rate. No throttling losses = better overall efficiency. **Up to 60% lower total losses!**

Variable speed pumping reduces losses



Source: Siemens AG, Pictures of the future

Variable speed elevators save energy

Elevator:

1 Ton pay-load, 17 m delivery head, 5 stops

- a) **Old drive:**
- Fixed speed drive at the grid: 8.8 kW-induction motor,
 - Speed variation by pole-changing („slow-fast“)
 - Standard gear
 - Mechanical braking during stops (Braking energy as heat)
- b) **New drive:**
- 7.5 kW induction motor with raised efficiency
 - Speed variation via inverter-feeding
 - Low loss gear with synthetic oil
 - Energy recovery during braking via the inverter (with Active Front End)

Total energy saving per ride: 81 % at full load (best case)

Pay-back time for the more expensive “New drive” 5.5 years at a rate of 400 daily rides!

Source: ZVEI, Frankfurt, Germany



5. Inverter-fed induction machines

5.3 Features of special induction motors for inverter operation



Source:
ELIN EBG Motoren
GmbH, Austria

Induction motor design: Grid vs. inverter-operation

- Equivalent circuit motor parameters for line- vs. inverter operated induction machines

<i>Aim Grid / Inverter</i>	<i>air gap</i>	<i>L_σ</i>	<i>R_r</i>
Big breakdown torque	-	small	-
Small magnetizing current	small	-	-
low starting current	-	big	big
big starting torque	-	small	big
Low additional losses	big	big	small

- **Low leakage:** many slots, no skew, no deep slots, big slot openings
- **Small magnetizing current:** small air-gap, low iron saturation

Line-operation:

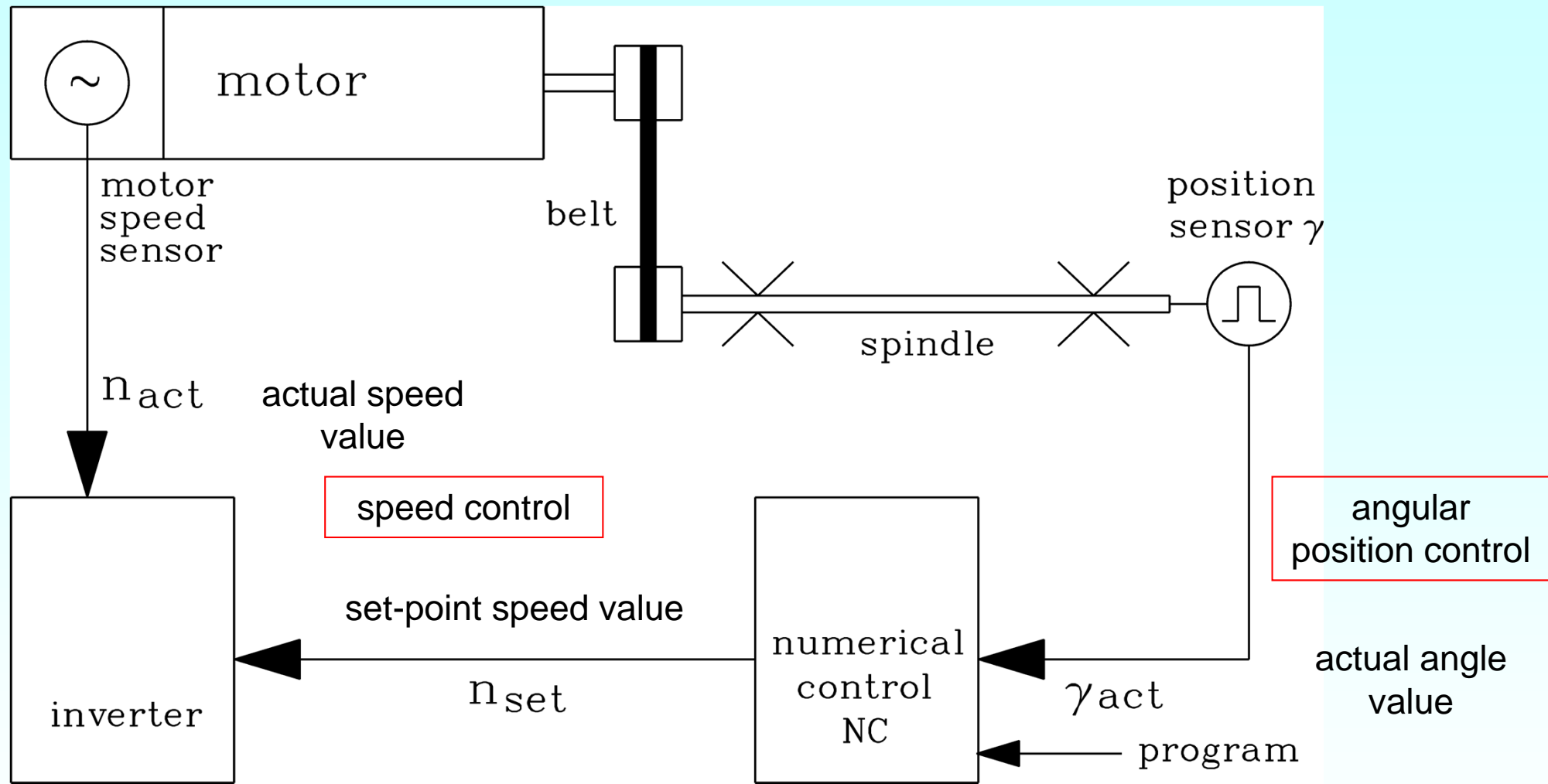
- **Big starting torque:** big current displacement, deep rotor slots, special rotor cage
- **Good starting performance:** skewing is necessary to minimize harmonic torque.

Inverter operation:

- **Small current displacement:** round or oval rotor slots
- **Low additional losses:** Avoid skewing to avoid inter-bar currents.
- **Sufficient leakage:** small slot openings, stray inductance must limit current harmonics.

$$M_b = \frac{m_s}{2} \frac{p}{\omega_s} U_{s,\max}^2 \frac{1-\sigma}{\sigma \omega_s L_s} \sim 1/\omega_s^2$$

Tooling machine: Variable speed main spindle drive



Source:
Siemens AG

- **Belt** as mechanical gear for big torque at the spindle at low speed

Increase of constant power range by switching a mechanical gear

Example:

$$i = 4:$$

$$n_N = 500/\text{min}$$

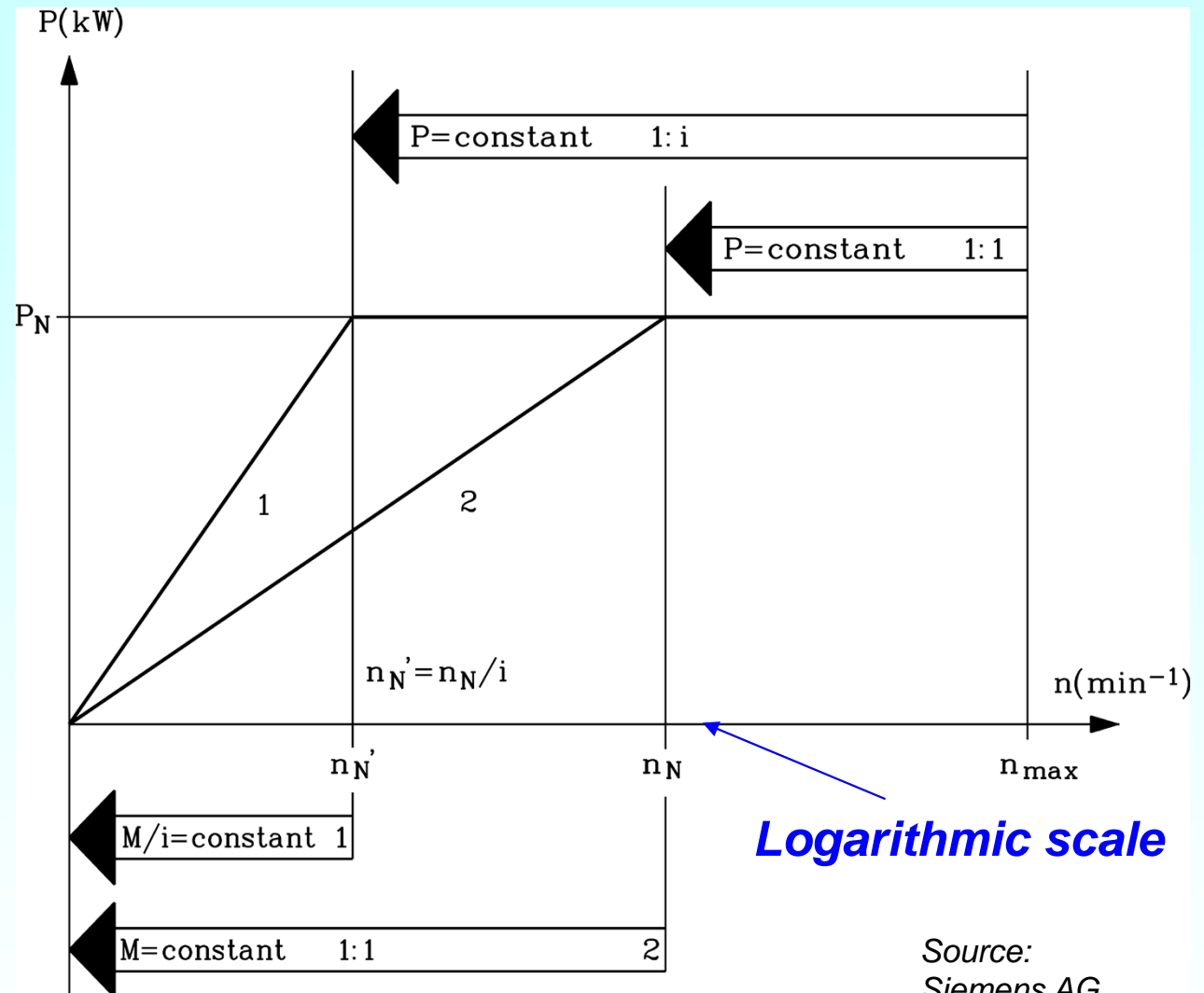
$$n_{\text{max}} = 7500/\text{min}$$

$$n'_N = 125/\text{min}$$

Extension of constant power range from

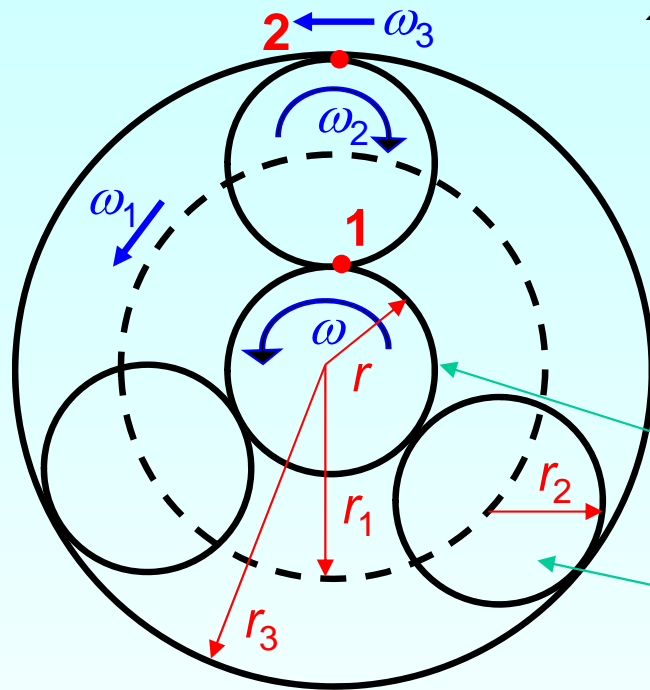
$$500 \dots 7500 = 1:15$$

$$\text{to } 125 \dots 7500/\text{min} = 1:60$$



- **Gear transfer ratio $i > 1$:** Increase of constant power range at low speed e.g. $i = 4$

Planetary gear



$$\left. \begin{array}{l} 1: \omega \cdot r = \omega_1 \cdot r_1 + \omega_2 \cdot r_2 \\ 2: \omega_3 \cdot r_3 = \omega_1 \cdot r_1 - \omega_2 \cdot r_2 \end{array} \right\} \omega_1 = \frac{\omega \cdot r + \omega_3 \cdot r_3}{2 \cdot r_1} \quad i = \frac{\omega_1}{\omega} = \frac{r + r_3 \cdot (\omega_3 / \omega)}{2 \cdot r_1}$$

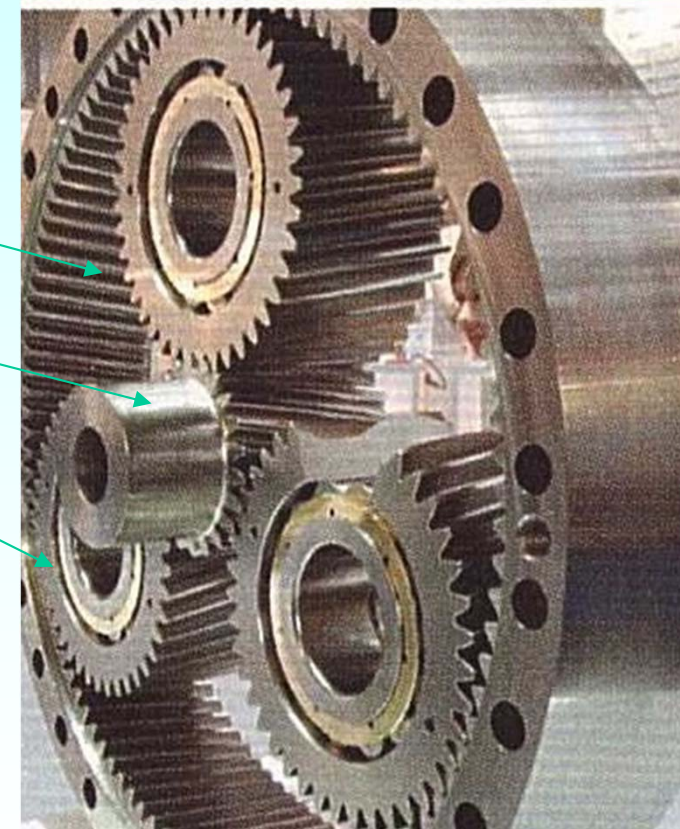
Case I: $\omega_3 = 0: i = \frac{r}{2r_1}$

Case II: $\omega_3 = \omega: i = \frac{r}{2r_1} + \frac{r_3}{2r_1}$

hollow wheel

sun wheel

planetary wheel



Source: NKE, Germany

Special case:

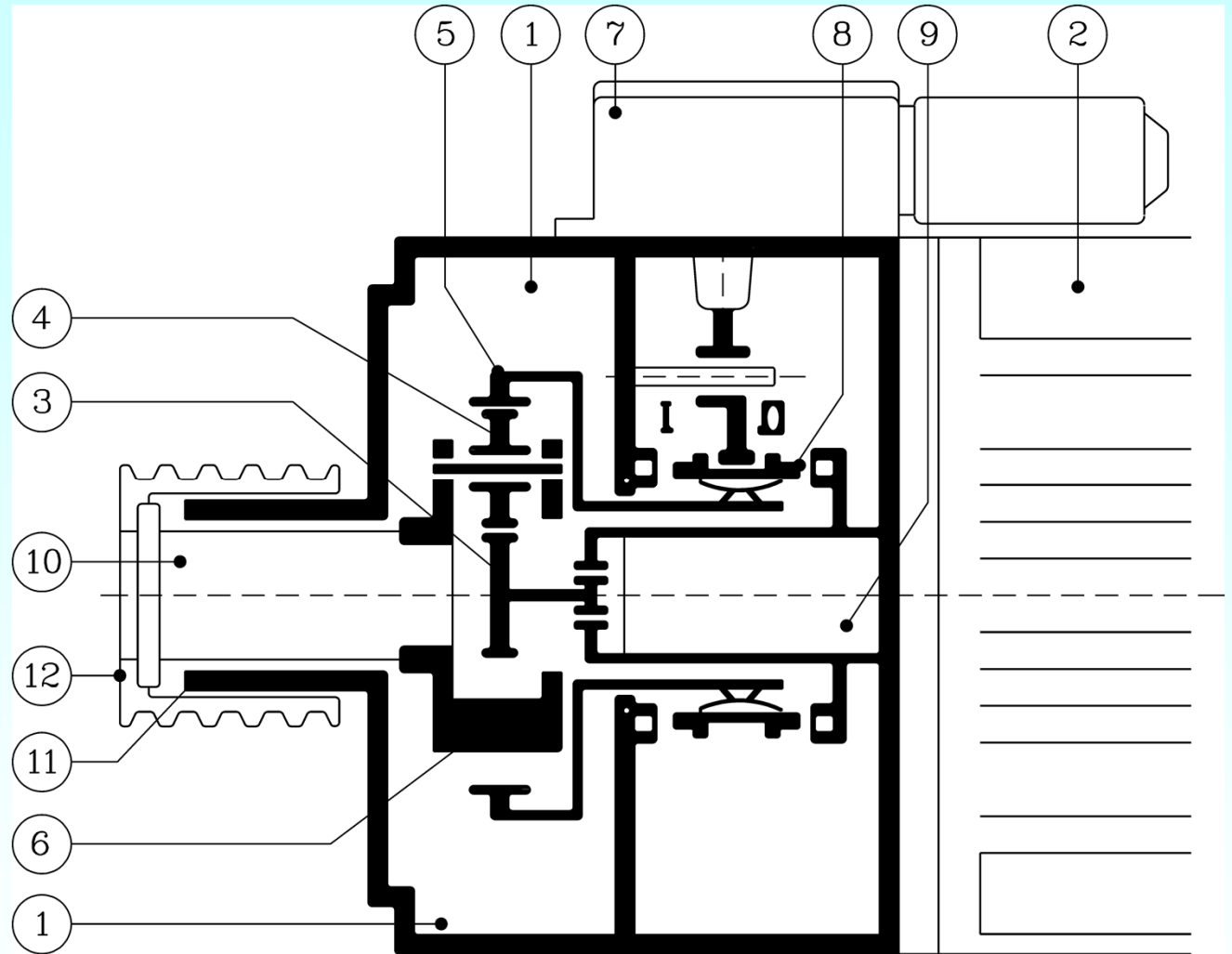
$$r_2 = r \rightarrow r_1 = 2r, \quad r_3 = 3r$$

Case I: $\omega_3 = 0: i = \frac{1}{4}$

Case II: $\omega_3 = \omega: i = \frac{1}{4} + \frac{3}{4} = 1$

Switching planetary gear with $i = 1$ and $i = 4$

- 1: gear housing 2: motor
- 3: sun wheel
- 4: planetary wheel
- 5: hollow wheel
- 6: planetary wheel support
- 7: switching unit
- 8: shifting sleeve
- position I: gear ratio $1: i$,
position II: gear ratio $1: 1$
- 9: motor shaft 10: gear shaft
- 11: housing 12: belt pulley



The motor has a holding brake at switched-off power.

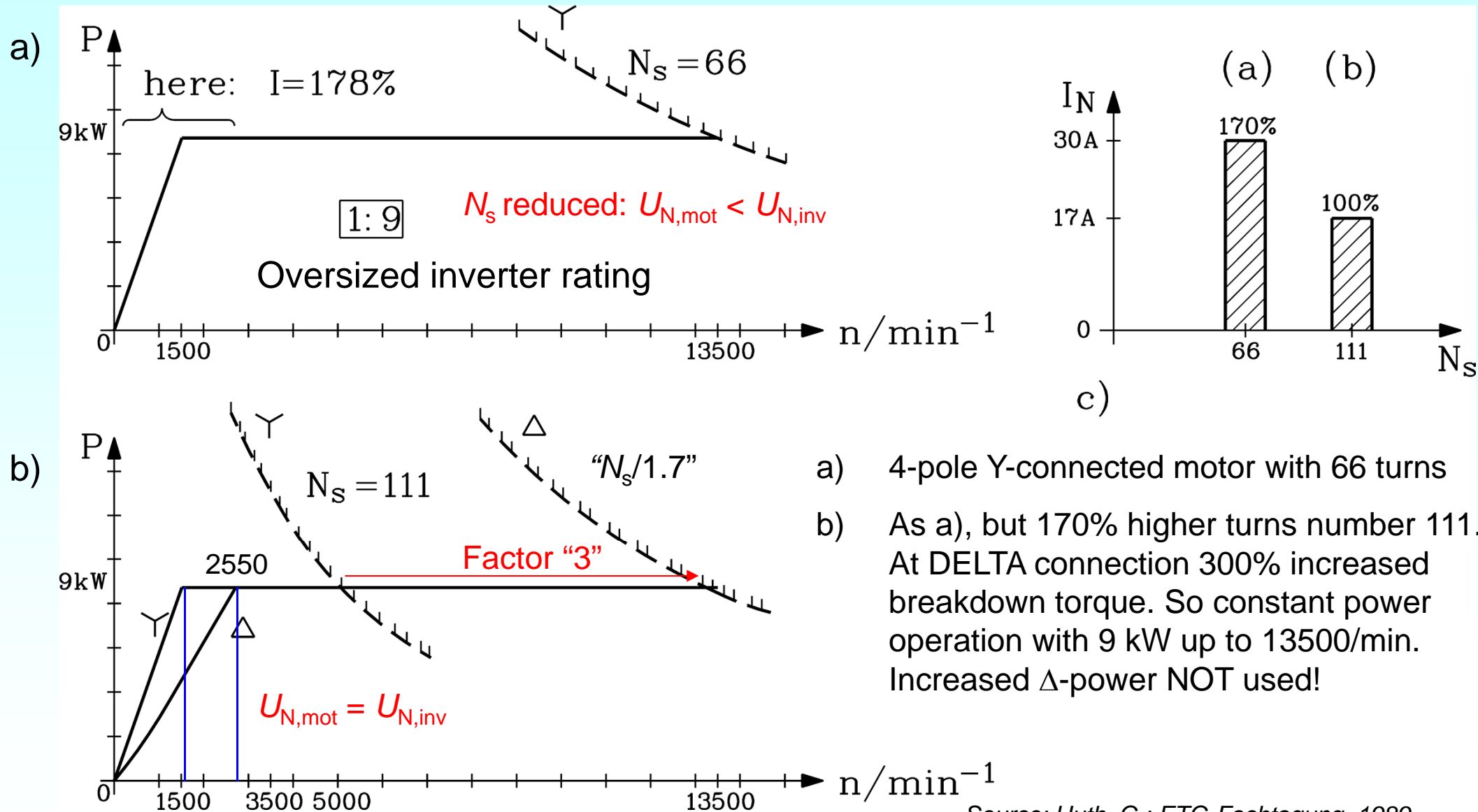
Source:
Siemens AG

Induction motors for wide field weakening range

- Over-sizing of motor: M_b/M_N increased
- Increase of inverter current rating I_s : N_s reduced,
 $I_s N_s = \text{const.}$ for constant rated torque
= increased conductor cross section A_c at constant current density $J_s = I_s/A_c$ (slot fill factor $k_Q = N_c A_c/A_Q = \text{const.}$, inductance $L_s \sim (N_s)^2$ decreased, $M_b \sim 1/L_s$ increased
- Star-delta switching of stator winding
- Series-parallel switching of stator winding



Star-delta switching of stator winding for same motor volume to increase constant power range by 1:3



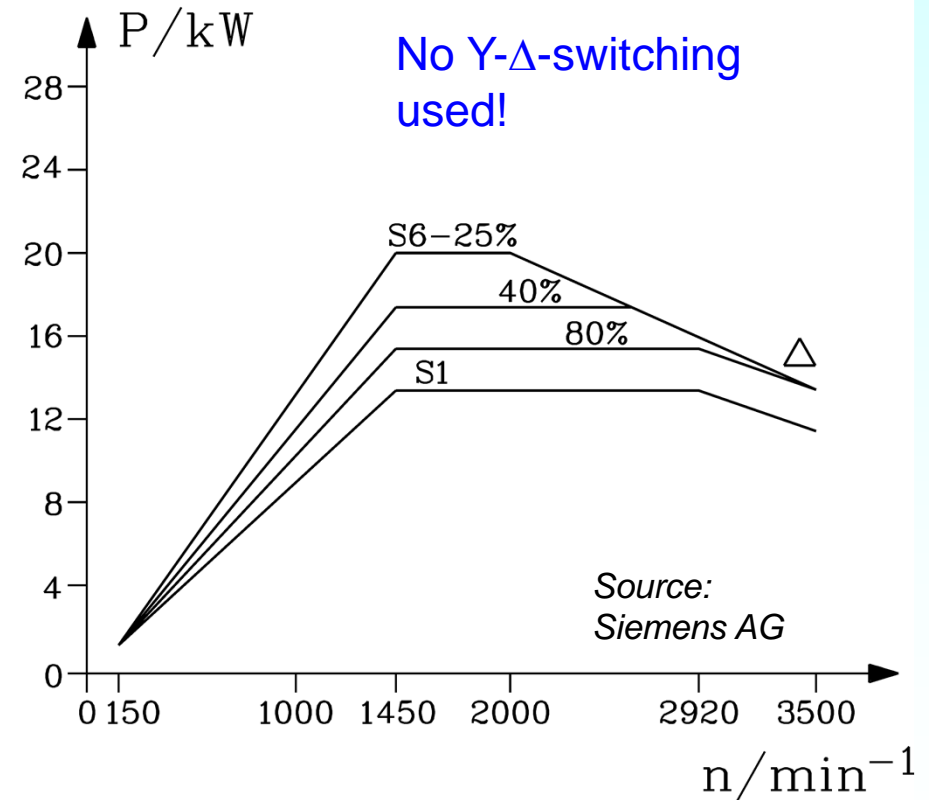
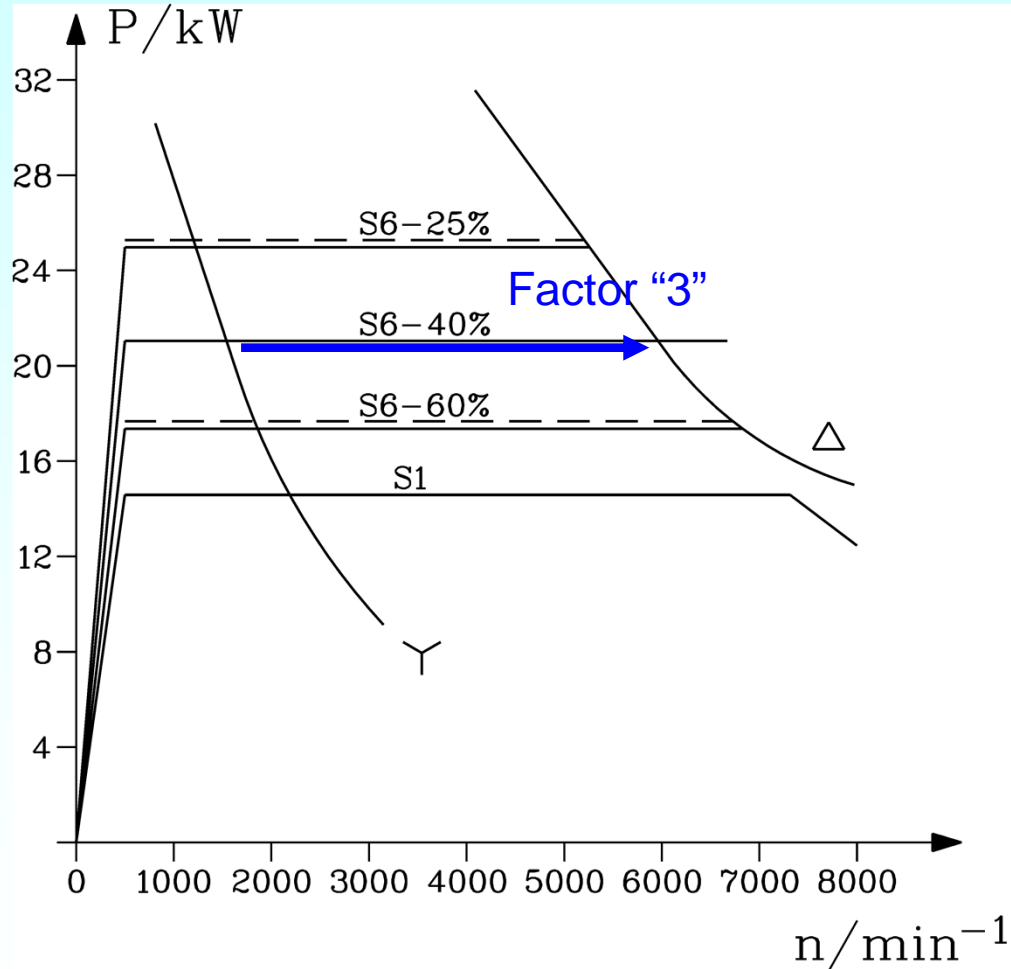
- a) 4-pole Y-connected motor with 66 turns
- b) As a), but 170% higher turns number 111. At DELTA connection 300% increased breakdown torque. So constant power operation with 9 kW up to 13500/min. Increased Δ -power NOT used!

Source: Huth, G.; ETG-Fachtagung, 1989

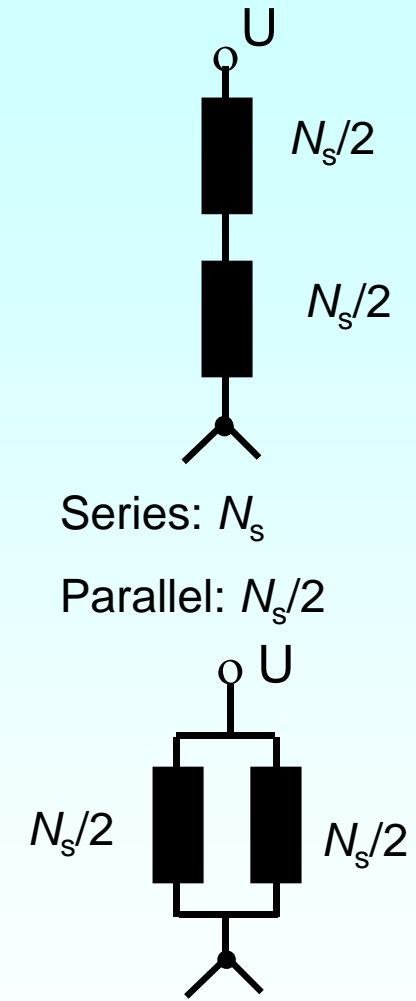
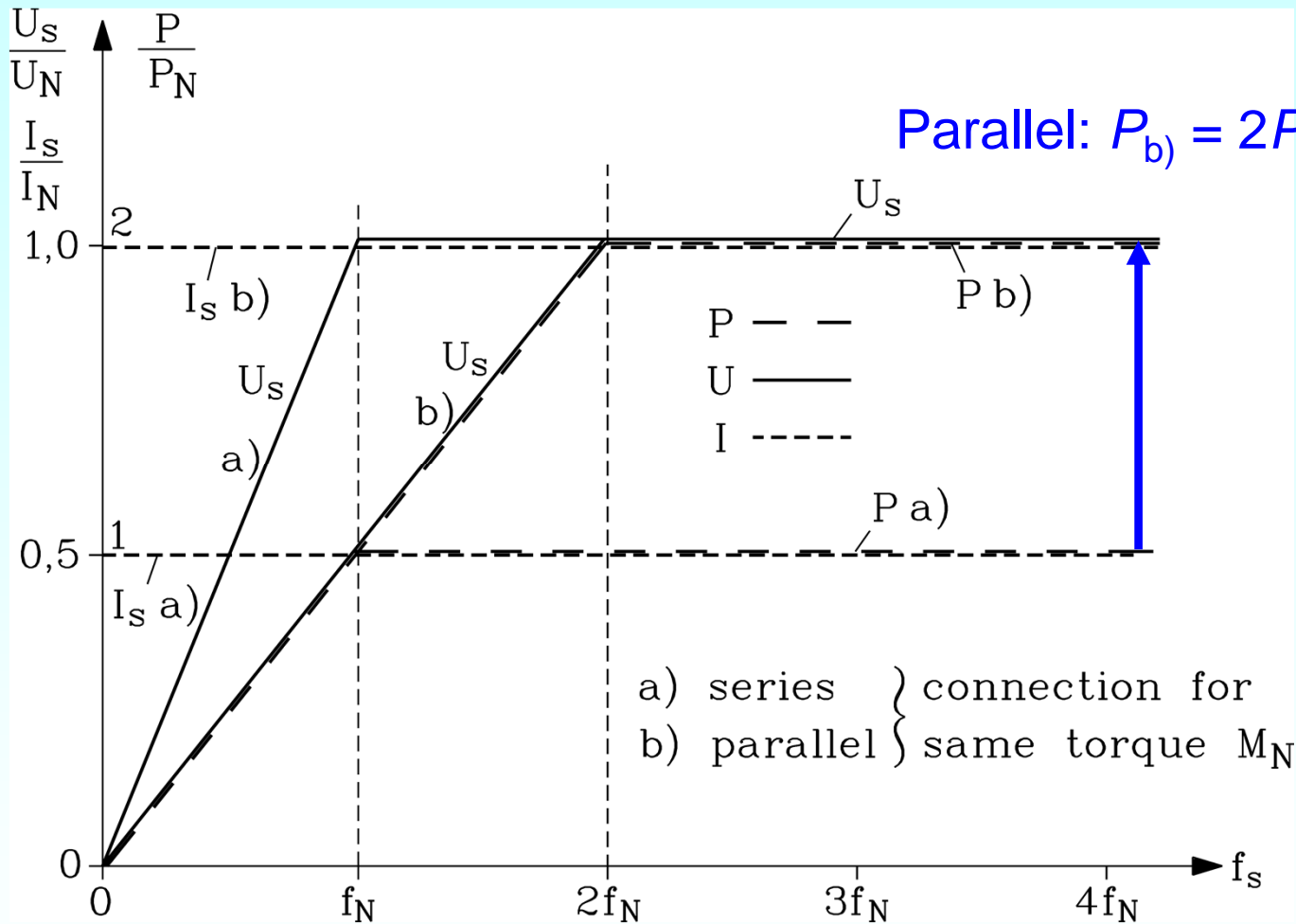
Series-parallel switching of stator winding

High performance 4-pole induction motor with star-delta switch to enlarge constant power range, rated speed at Y: 500/min, rated frequency 16.7 Hz

Standard induction 4-pole motor, D connected winding, rated speed 1460 /min, rated frequency 50 Hz

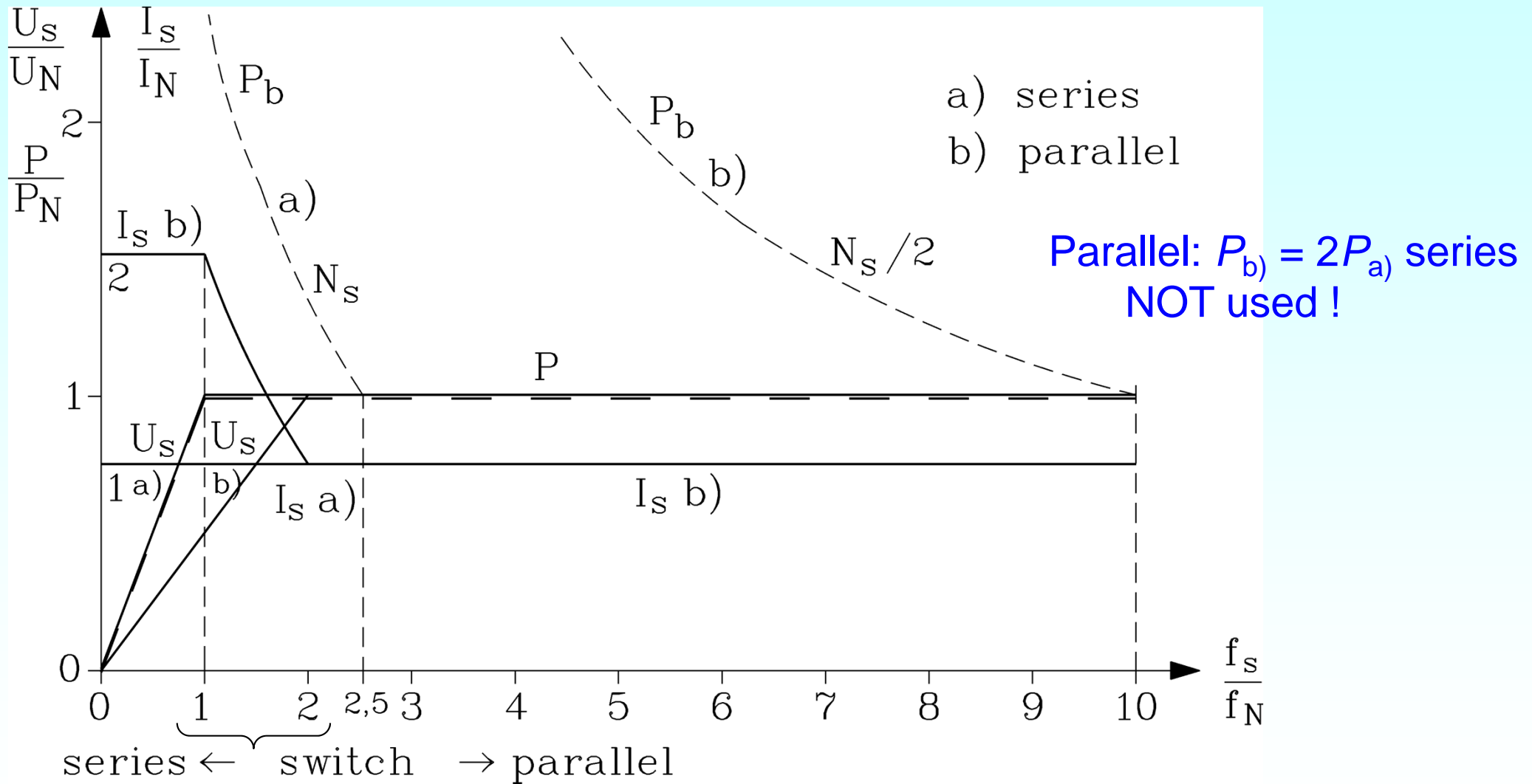


Series-parallel switching of stator winding (1)



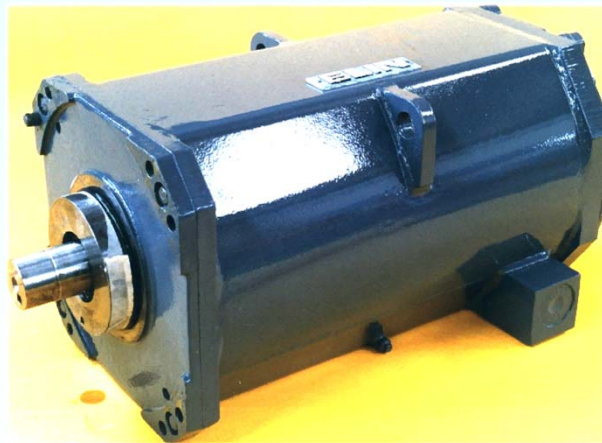
Series-parallel switching of stator winding (2)

- Increasing constant power range by factor 4
- Increase of field weakening by factor 4 from 1:2.5 to 1:10



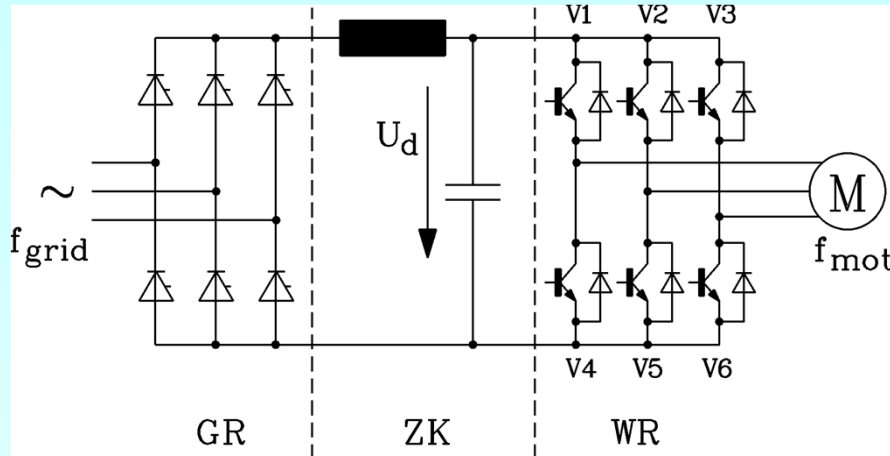
5. Inverter-fed induction machines

5.4 Influence of inverter harmonics on motor performance



Source:
ELIN EBG Motoren GmbH,
Austria

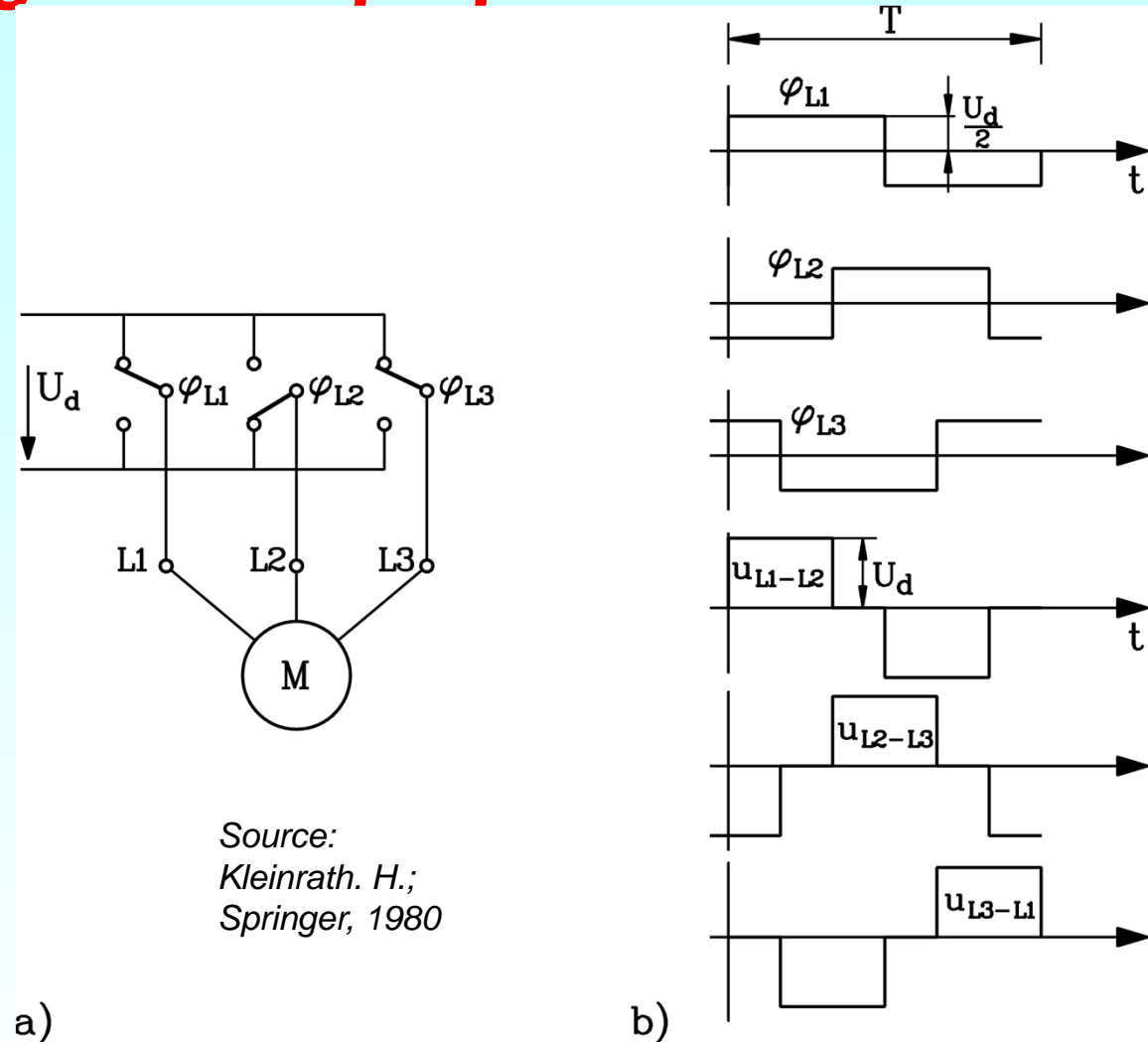
Inverter with voltage six step operation



- Bridge rectifier with thyristors on grid side GR (firing angle α) generates **variable DC voltage U_d** in DC link ZK; voltage smoothed by capacitor.

- Inverter WR generates by six-step switching from U_d a **block shaped** line-to-line output voltage between terminals L1, L2, L3.

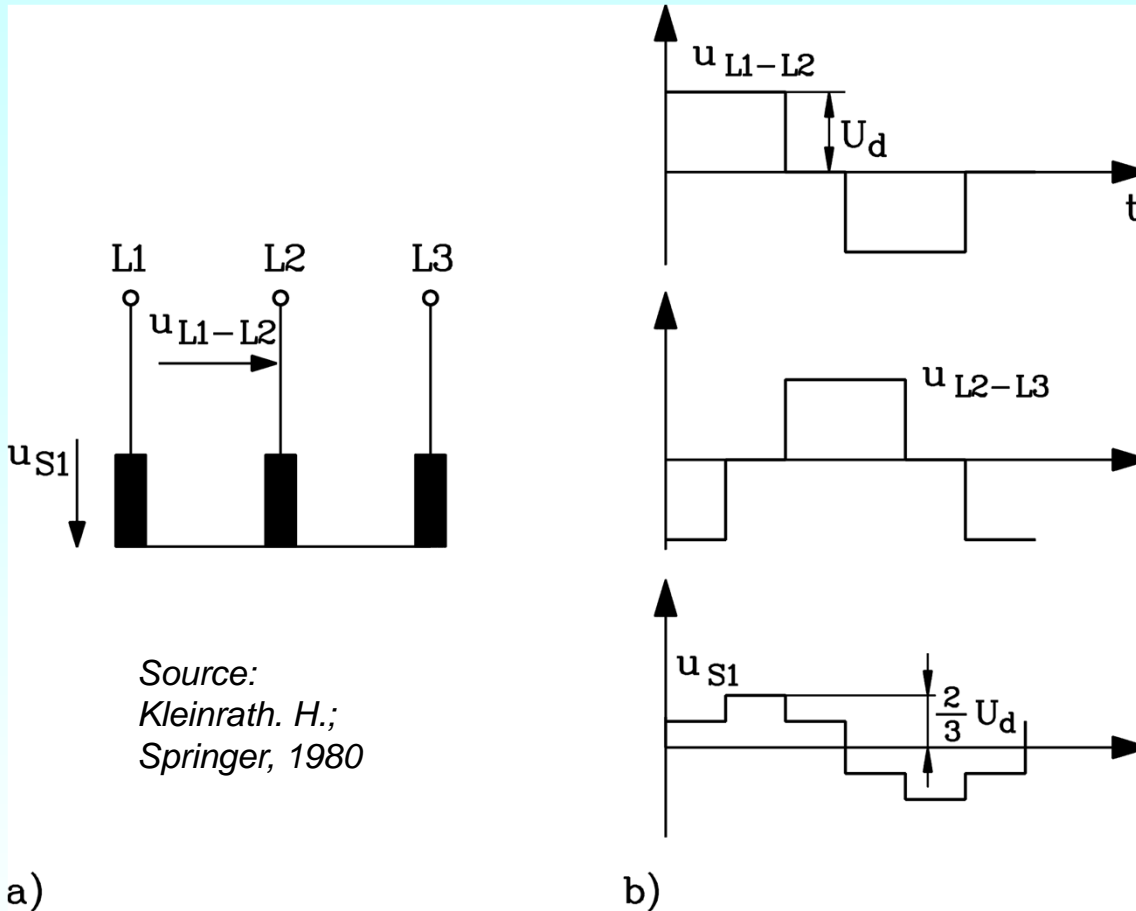
- DC link voltage U_d is changed by α **proportional** with output frequency $f_{\text{mot}} = 1/T$
- Grid side energy feed-back only possible with 2nd anti-parallel thyristor bridge: At $\alpha > 90^\circ$ positive U_d and negative I_d give **negative** dc link power = **power to the grid (gener. braking).**



Source:
Kleinrath, H.;
Springer, 1980

Voltage harmonics at six-step operation (see Chapter 1)

- Inverter output phase voltage: $u_{S1} - u_{S2} = u_{L1-L2}$; $u_{S2} - u_{S3} = u_{L2-L3}$; $u_{S1} + u_{S2} + u_{S3} = 0$;



we get:
$$u_{S1} = \frac{2u_{L1-L2} + u_{L2-L3}}{3}$$

- Block shaped line-to-line voltage, expanded as *FOURIER*-series:

$$u_L(t) = \sum_{k=1,-5,7,\dots}^{\infty} \hat{U}_{L,k} \cdot \cos(k \cdot \omega_s t)$$

$$k = 1 + 6g, \quad g = 0, \pm 1, \pm 2, \dots$$

$$\Rightarrow k = 1, -5, 7, -11, 13, \dots$$

$$\hat{U}_{L,k} = \frac{2}{\pi} \sqrt{3} \frac{U_d}{k}$$

Electrical machine is fed with a mix of harmonic voltages of different amplitude, frequency and phase angle. Only fundamental (ordinal number $k = 1$) is desired. Voltage harmonics ($|k| > 1$) cause harmonic currents in electric machine with additional losses, torque pulsation, vibrations and acoustic noise.

Harmonic voltage systems (see Chapter 1)

$k = 1$:

$$u_{U1}(t) = \hat{U}_1 \cdot \cos(\omega t)$$

$$u_{V1}(t) = \hat{U}_1 \cdot \cos(\omega t - 2\pi / 3)$$

$$u_{W1}(t) = \hat{U}_1 \cdot \cos(\omega t - 4\pi / 3)$$

U – V – W

Positive sequence system

$k = 5 \Rightarrow k = -5$:

$$u_{U5}(t) = \hat{U}_5 \cdot \cos(5\omega t)$$

$$u_{V5}(t) = \hat{U}_5 \cdot \cos(5(\omega t - 2\pi / 3)) = \hat{U}_5 \cdot \cos(5\omega t + 2\pi / 3)$$

$$u_{W5}(t) = \hat{U}_5 \cdot \cos(5(\omega t - 4\pi / 3)) = \hat{U}_5 \cdot \cos(5\omega t + 4\pi / 3)$$

U – W – V

Negative sequence system

- General rule:** Positive and negative systems occur alternatively: Ordinal number k has a positive or negative sign: $k = +1, -5, +7, -11, +13, \dots$

$$u_{Uk}(t) = \hat{U}_k \cdot \cos(k\omega t)$$

$$u_{Vk}(t) = \hat{U}_k \cdot \cos(k\omega t - 2\pi / 3)$$

$$u_{Wk}(t) = \hat{U}_k \cdot \cos(k\omega t - 4\pi / 3)$$

$$k = 1 + 6g$$

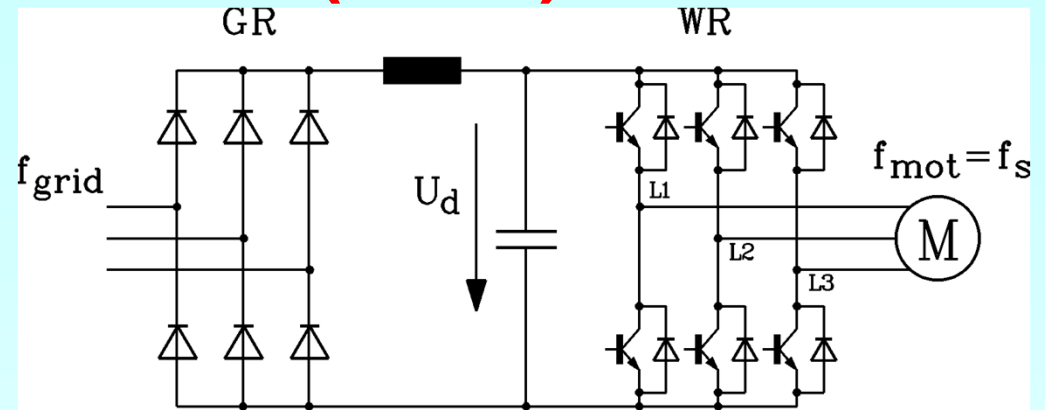
$$g = 0, \pm 1, \pm 2, \dots$$

Pulse width modulation (PWM)

- At grid side: Diode rectifier GR (= firing angle $\alpha = 0$): generates **constant DC link voltage** U_d , which is smoothed by capacitor:

$$U_d \sim U_{grid} = const.$$

- Motor side inverter WR generates from U_d **by pulse width modulation** a line-to-line voltage between L1, L2, L3. Width of pulses is defined by comparison of **saw tooth signal** u_{sz} (switching frequency f_{sch}) with AC **reference signal** u_{ref} , which pulsates with desired **stator frequency** f_s . With comparator a **PWM-signal** is generated to control power switches. *Reference signal is most often sine wave.*
- Amplitude A_1 of u_{ref} defines amplitude of fundamental of PWM voltage at motor terminal. So it is varied **proportional** to f_{mot} .
- Grid side: $\cos \varphi = 1$ **No power flow back into grid possible.** (For that a grid-side inverter and a grid-side inductance is necessary !). Therefore generator braking power has to be dissipated in "brake"-**resistors, which are connected in parallel** with capacitor in DC link.



Generation of PWM voltage

- a) Comparison of saw tooth and reference signal lead to PWM control signal for power switches: Potential $\varphi_{L1}(t)$ at terminal L1 varies with that PWM signal
- b) Difference of two terminal potentials delivers line-to-line voltage $u_{L1-L2}(t)$

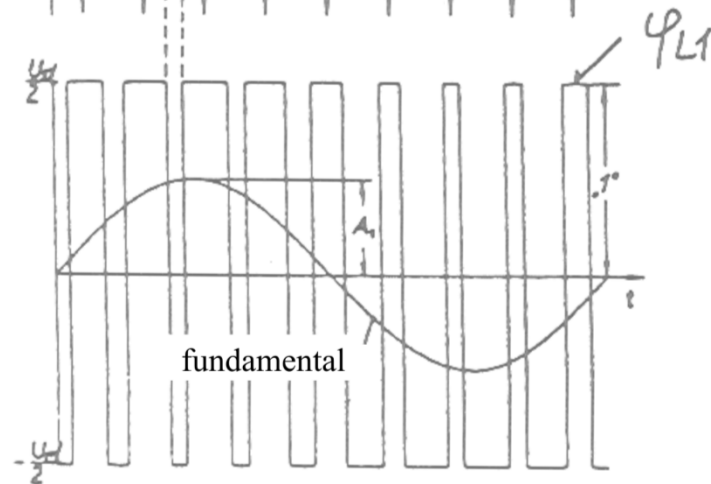
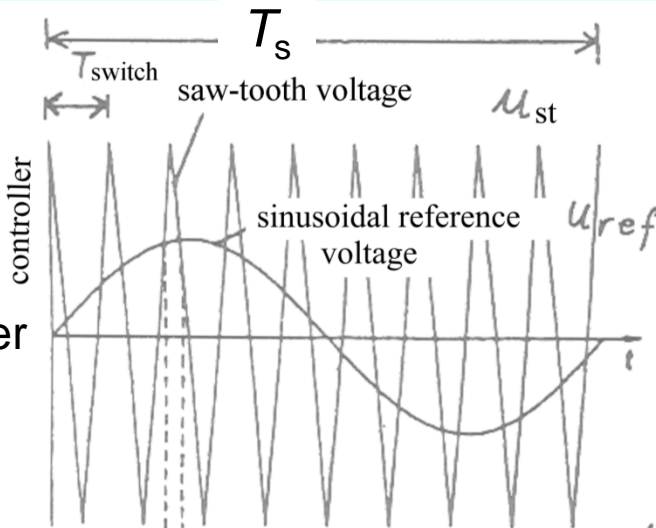
Example:

Synchronous switching mode

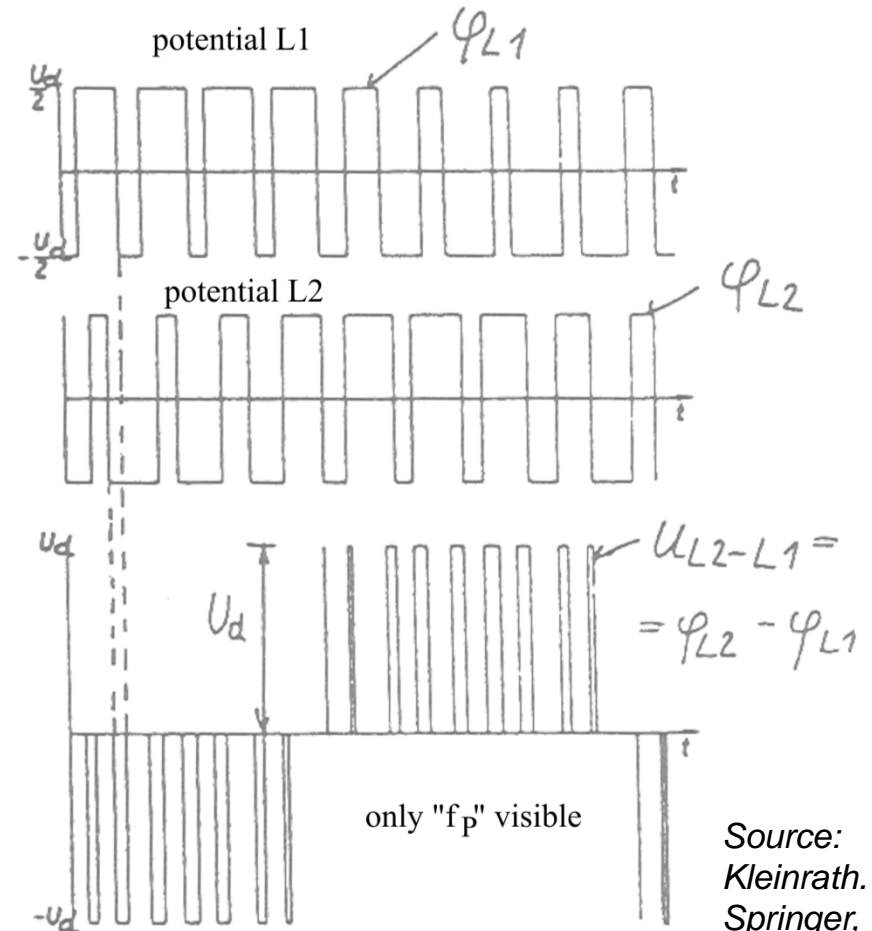
$T_s / T_{\text{switch}} = \text{integer}$

$f_s = f_{\text{mot}} = 1/T_s$

$f_T = 1/T_{\text{switch}}$



a) $m = A_1 = \hat{U}_{\text{phase}} / (U_d / 2)$ modulation degree



$f_p = 2/T_{\text{switch}}$

Source:
Kleinrath. H.;
Springer, 1980

Voltage harmonics: Six-step and PWM

- **Six-step modulation:** FOURIER spectrum of line-to-line inverter output voltage:

k	1	-5	7	-11	13
$\hat{U}_{Lk} / \hat{U}_{L1}$	1	-0.2	0.14	-0.1	0.08

- **PWM:** FOURIER spectrum of terminal electric potential $\varphi_{L1}(t)$ and of line-to-line voltage $u_{L1-L2}(t)$ (at modulation degree $m = A_1 = 0.5$ and switching frequency ratio $f_T/f_s = 9$)

$ k $	1	3	5	7	9	11	13	15	17	19
$\hat{\varphi}_k / (U_d / 2)$	0.5	$< 10^{-5}$	0.001	0.09	1.08	0.09	0.002	0.04	0.36	0.36
$\hat{U}_{L,k} / \hat{U}_{L,k=1}$	1	0	0.002	0.18	0	0.18	0.004	0	0.72	0.72

Spectrum of terminal potential φ_L shows big amplitude of fundamental, of switching harmonic ($k = 9$) and at **about twice switching frequency** $f_p = 2 f_T$ ($k = 17$ and 19).

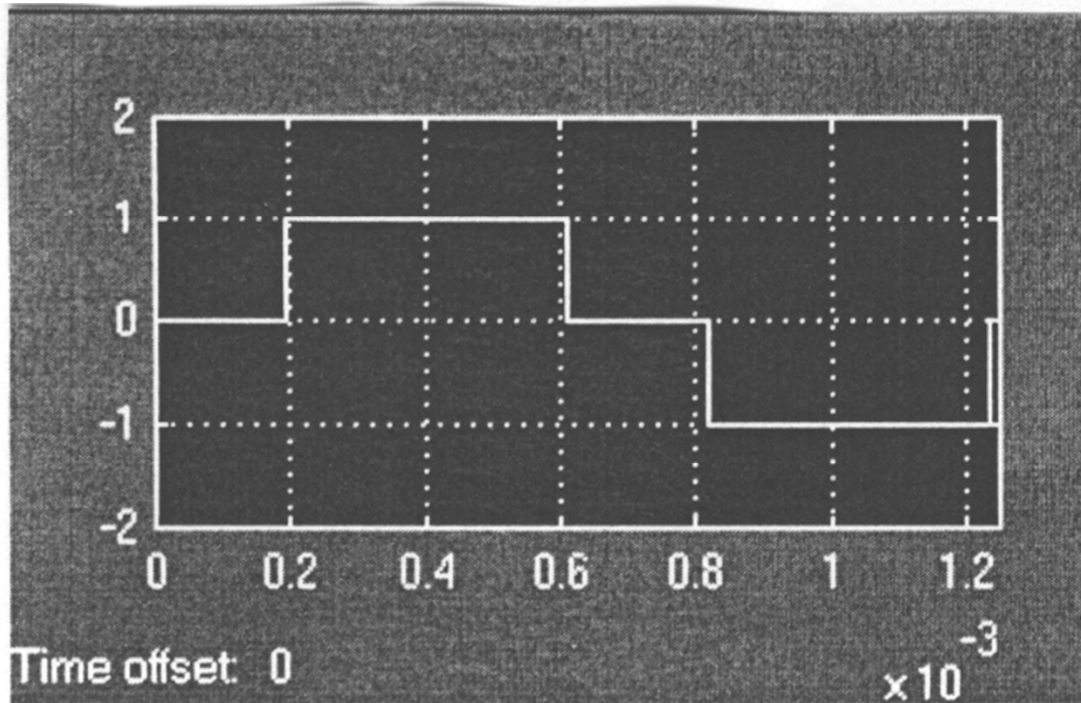
$$k = \left| \frac{f_p}{f_s} \pm 1 \right| \Rightarrow k = |18 \pm 1| = 17, 19$$

Voltage harmonics with ordinal numbers, divisible by 3, do **not** occur in line-to-line voltage, because f_T/f_s is divisible by 3 !

At high switching frequency f_T the amplitudes of all low voltage harmonics $f_k < f_T$ are small.

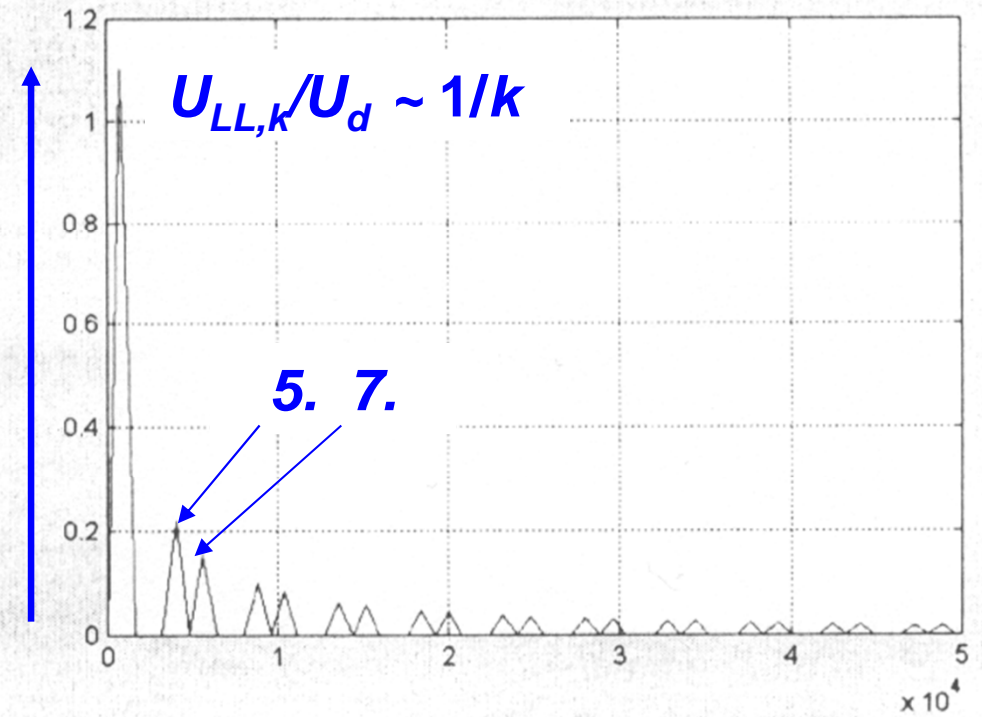
FOURIER-Spectrum of voltage harmonics: Six-step operation

u_{LL}/U_d



$f_s = 800 \text{ Hz}$

t / s



f / Hz

Source:

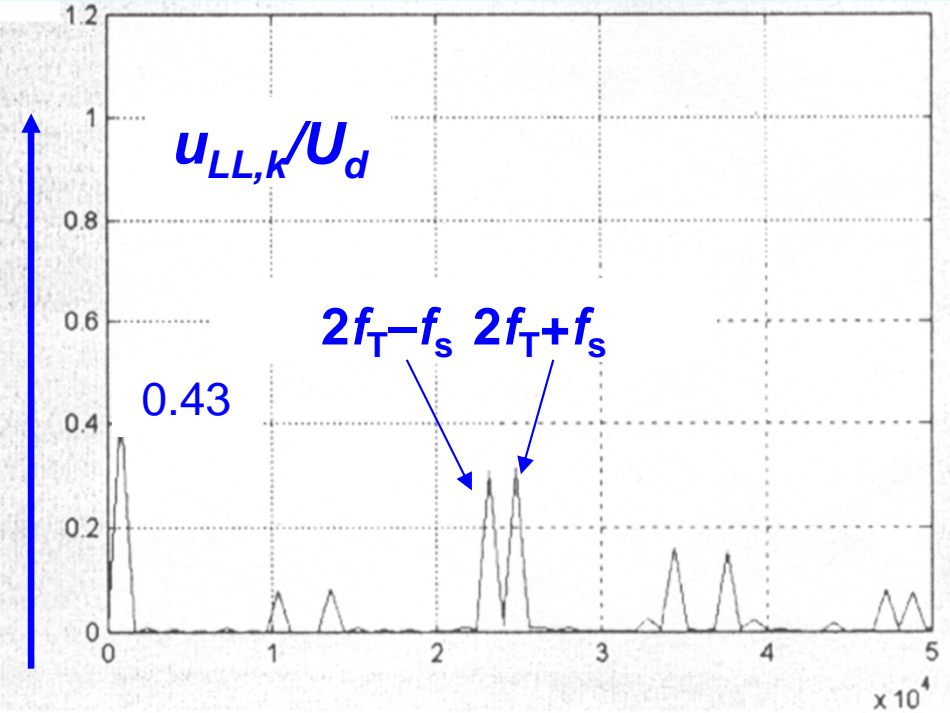
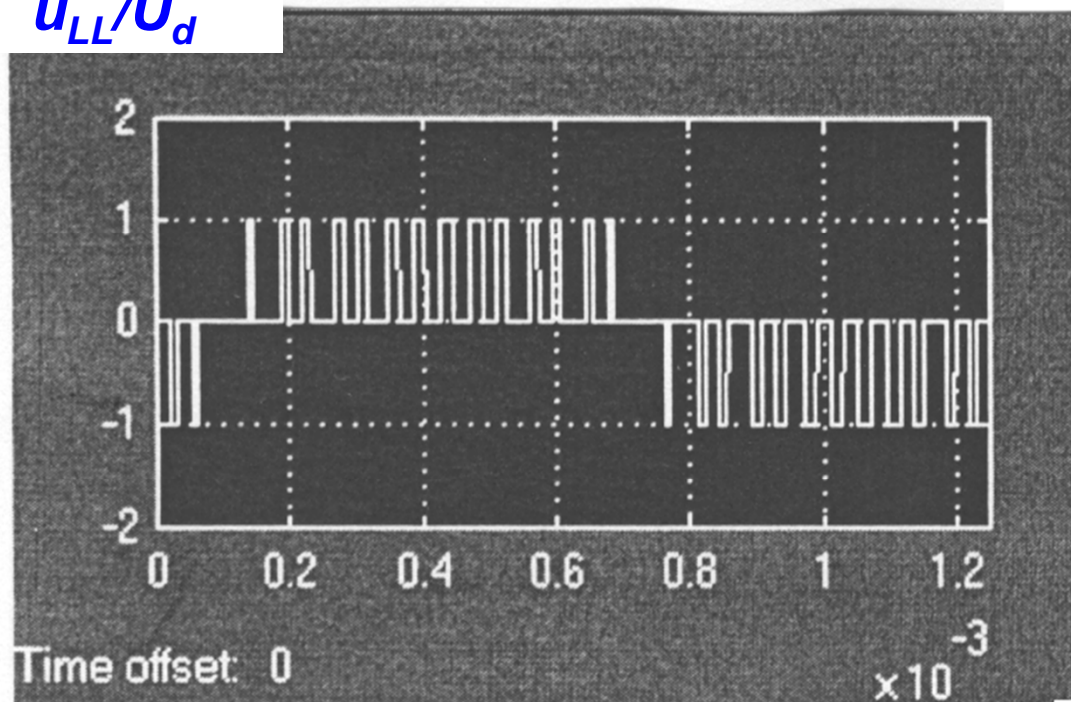
T. Lu, PhD Thesis, TU Darmstadt, 2004



FOURIER-Spectrum of voltage harmonics: PWM at 50% modulation degree

$$k = 1 : m = \hat{U}_{phase,1} / (U_d / 2) = 0.5 : \hat{U}_{LL,1} / U_d = \sqrt{3} \cdot m / 2 = 0.43$$

u_{LL}/U_d



t / s

f / Hz

Fundamental frequency $f_s = 800 \text{ Hz}$

Switching frequency $f_T = 12000 \text{ Hz} = 15f_s$

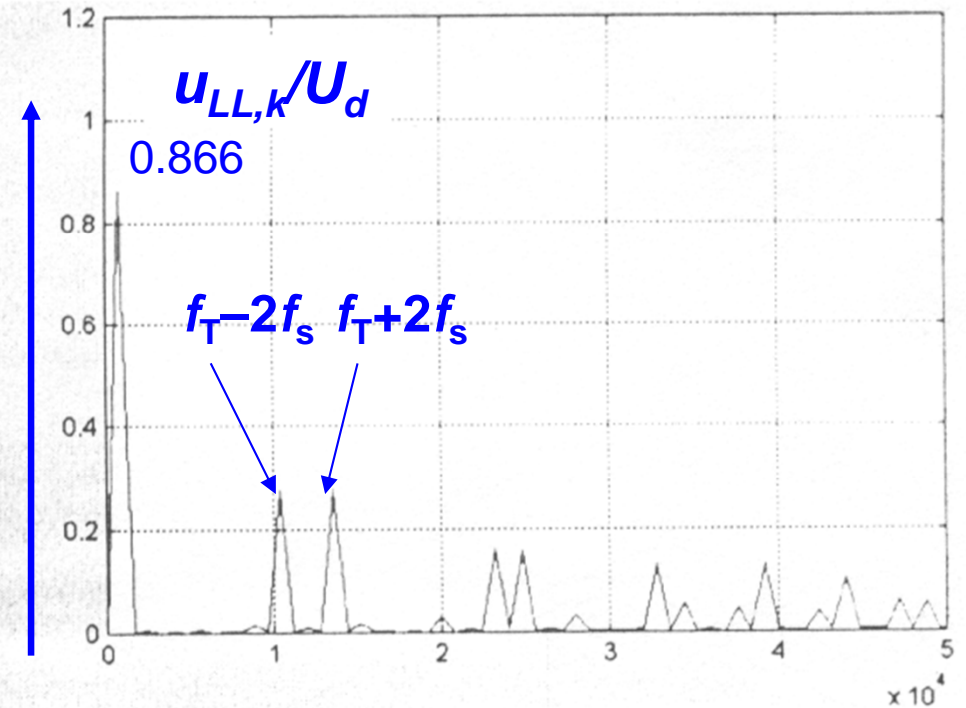
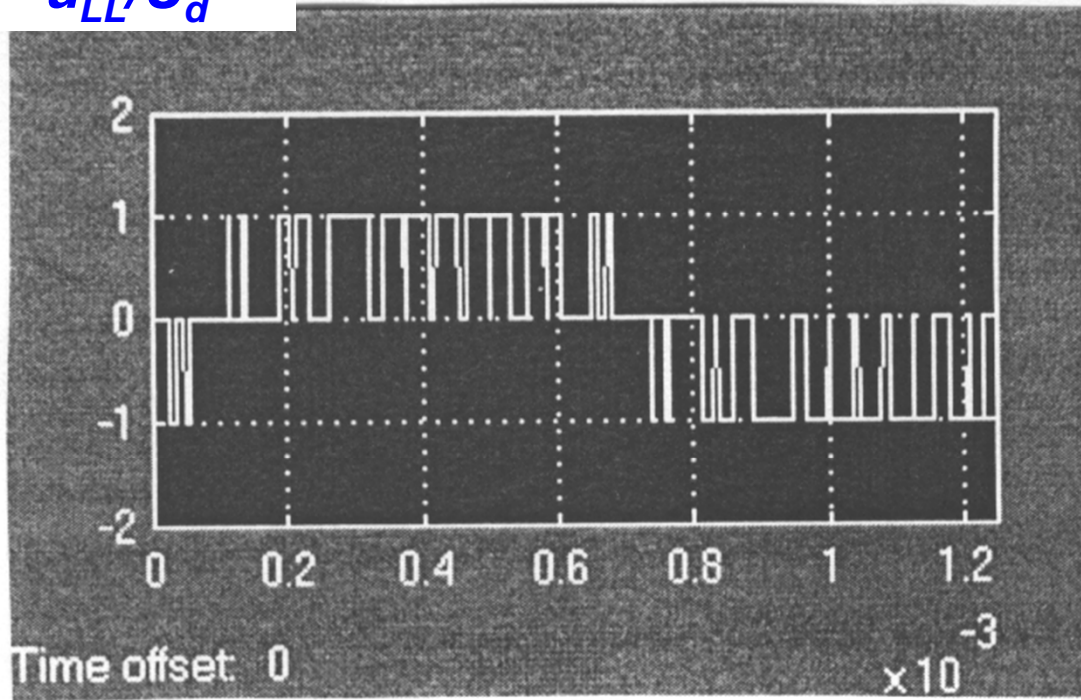
Source:

T. Lu, PhD Thesis, TU Darmstadt, 2004

FOURIER-Spectrum of voltage harmonics: PWM at 100% modulation degree

$$k = 1 : m = \hat{U}_{phase,1} / (U_d / 2) = 1 : \hat{U}_{LL,1} / U_d = \sqrt{3} \cdot m / 2 = 0.866$$

u_{LL}/U_d

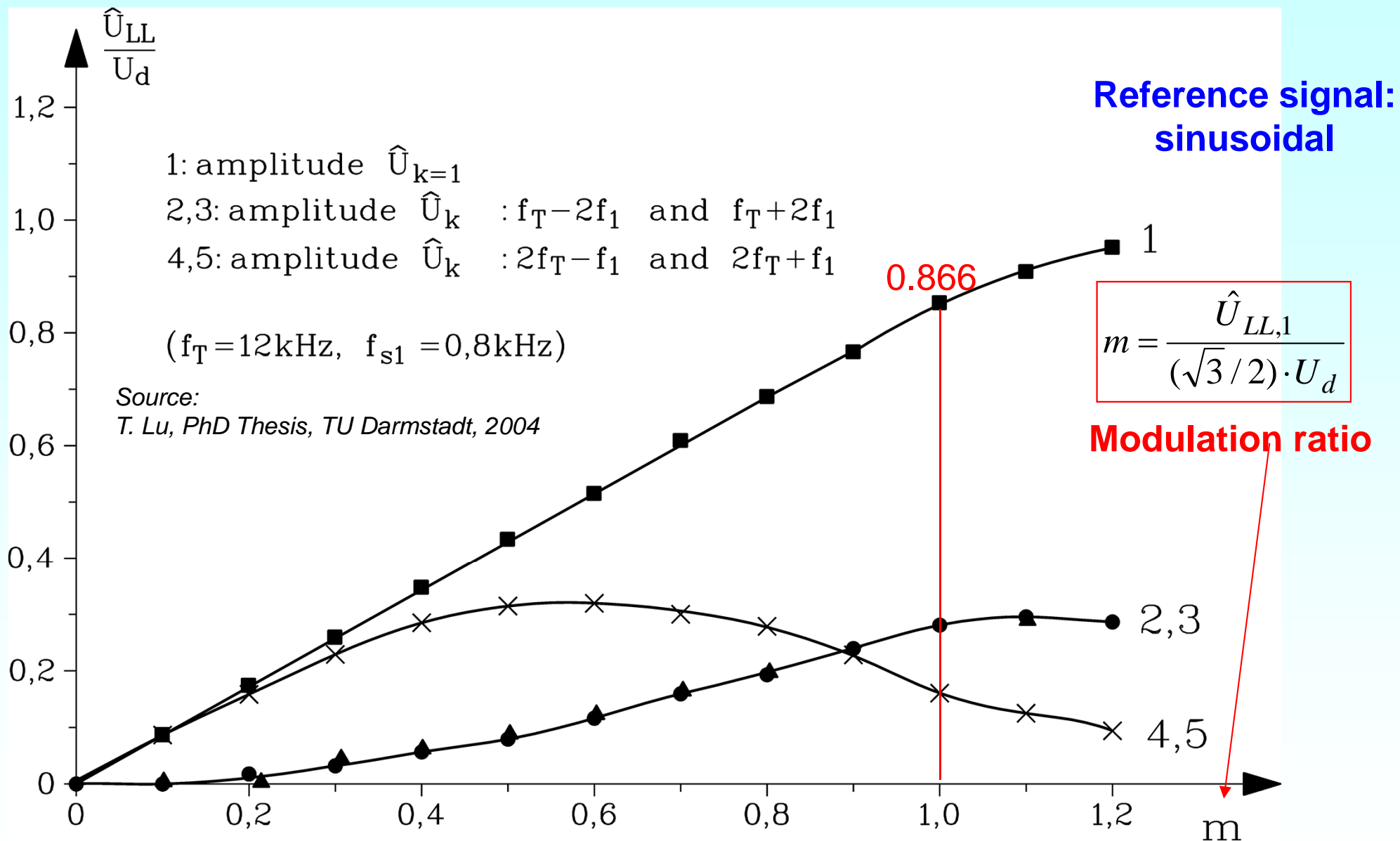


Fundamental frequency $f_s = 800$ Hz

Switching frequency $f_T = 12000$ Hz = $15f_s$

Source:
T. Lu, PhD Thesis, TU Darmstadt, 2004

Example: Voltage harmonics at “synchronous” PWM



Example: Current harmonics at PWM

Reference signal:
rectangular

Reference signal:
trapezoidal

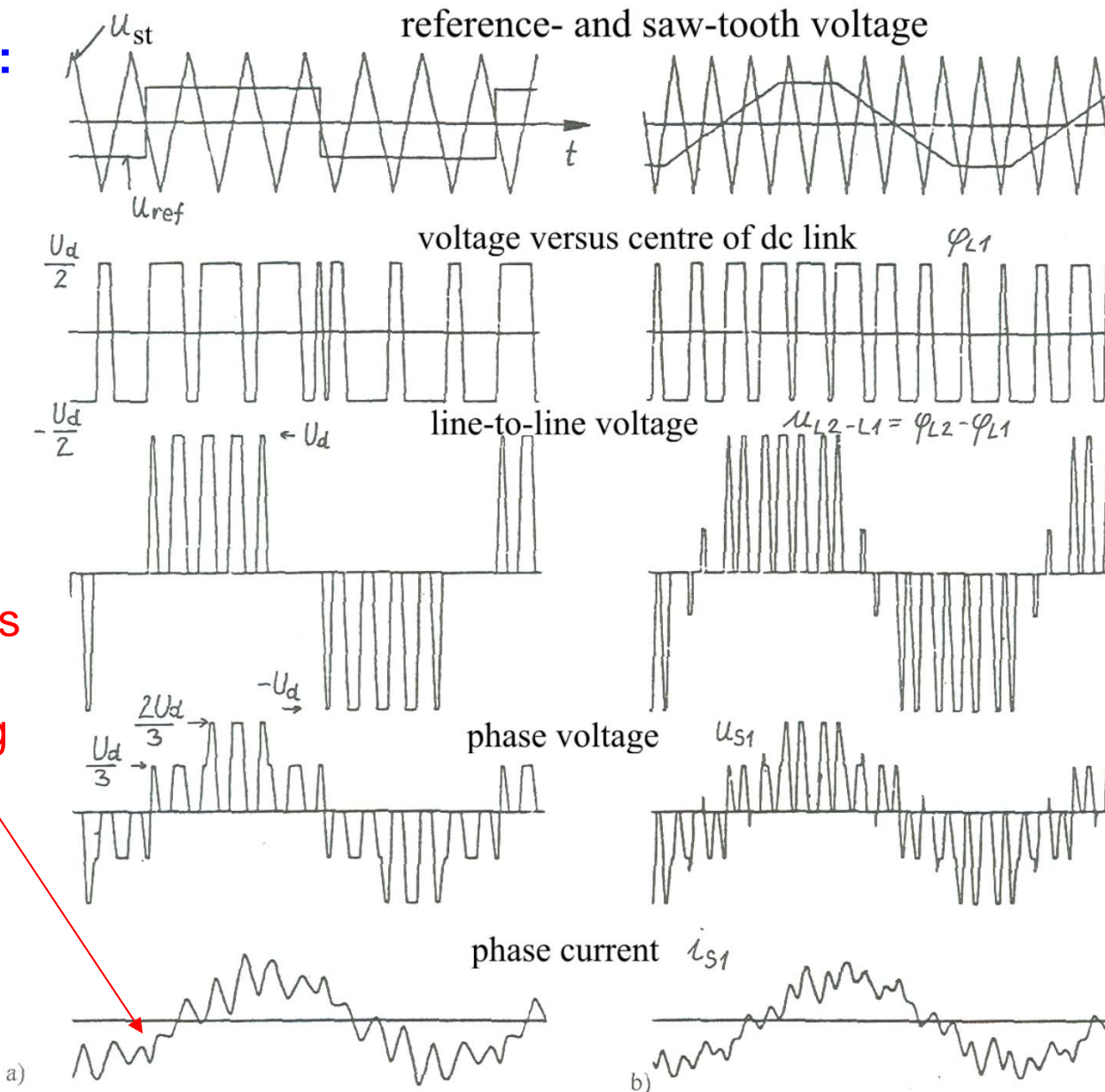
Current ripple
amplitude decreases
inverse with
increasing switching
frequency

Switching
ratio:

$$f_T/f_s = 6$$

Switching
ratio:

$$f_T/f_s = 9$$



Voltage harmonics cause current harmonics

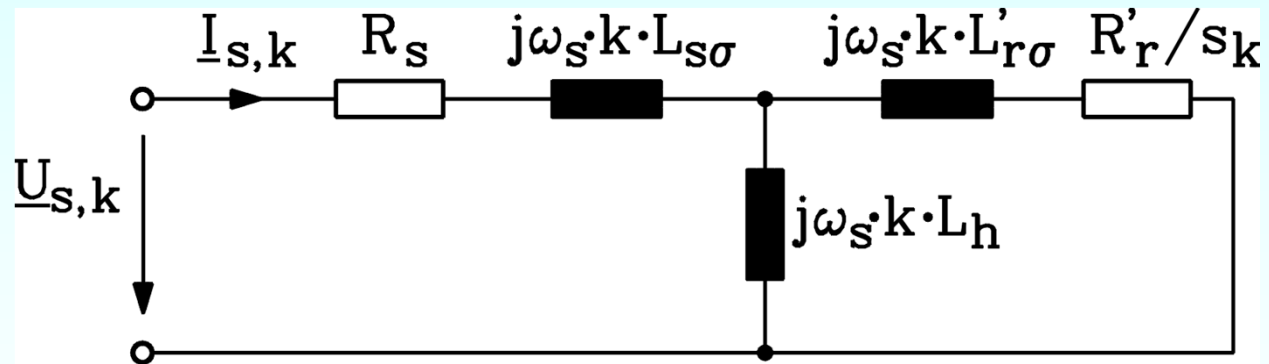
- The voltage harmonics per phase $U_{s,k}$ (frequency k -times fundamental frequency kf_s) cause current harmonics per phase $I_{s,k}$ in stator winding.
- These 3-phase harmonic current systems excite in the air gap a “high-speed” magnetic field wave (with pole count $2p$ due to the winding):

k^{th} synchronous velocity (“high speed”): $n_{syn,k} = k \cdot f_s / p$

- **Rotor slip with k^{th} high-speed field s_k :**

$$s_k = \frac{n_{syn,k} - n}{n_{syn,k}} = \frac{kn_{syn} - n}{kn_{syn}} = 1 - \frac{1}{k} \cdot \frac{n}{n_{syn}} = 1 - \frac{1}{k} \cdot (1 - s) \approx 1$$

As harmonic slips s_k are nearly unity, independent of base slip s , harmonic current amplitudes $I_{s,k}$ are nearly independent from load. Current harmonics are already present at no-load ($s = 0$) to full extent.



High speed fields $2p$ induce the rotor cage, causing rotor current harmonics with high frequency: $f_{rk} = s_k f_{s,k} \approx f_{s,k}$; causing big eddy currents in rotor bars and **big additional rotor losses !**

$$s_k \approx 1 \Rightarrow I_{s,k} \approx \frac{U_{s,k}}{\sqrt{(R_s + R'_r)^2 + (k\omega_s)^2 \cdot (L_{s\sigma} + L'_{r\sigma})^2}} \approx \frac{U_{s,k}}{|k|\omega_s(L_{s\sigma} + L'_{r\sigma})}$$

Example: Current harmonics at six-step modulation

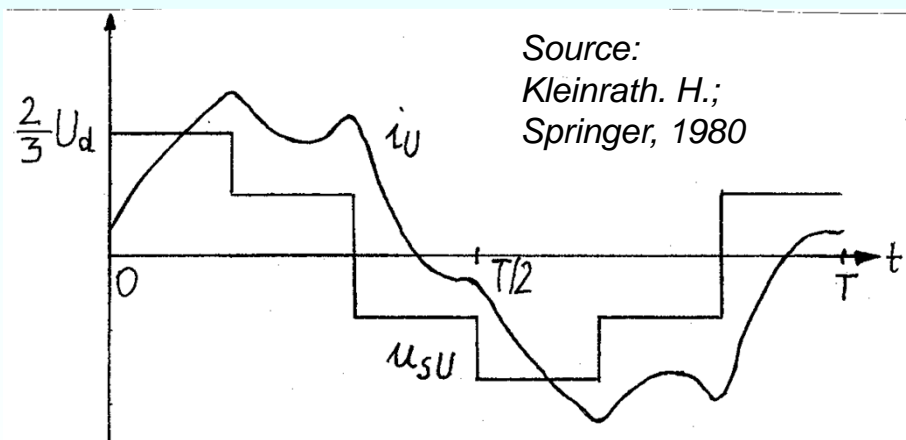
- Amplitudes of current harmonics at six step operation:

$$I_{s,k} \approx \frac{U_{s,k}}{|k|\omega_s(L_{s\sigma} + L'_{r\sigma})} \sim \frac{1}{|k|^2}$$

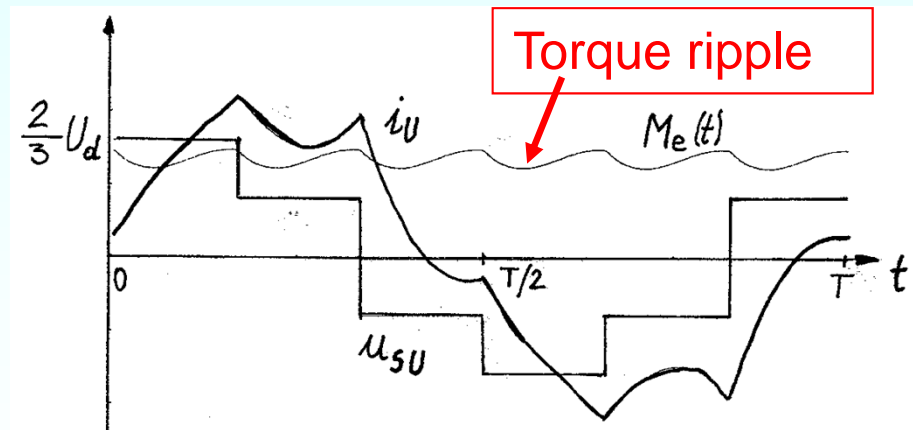
$$s = 1, s_k \approx 1:$$

k	1	-5	7	-11	13
$ \hat{U}_{Lk} / \hat{U}_{L1} $	1	0.2	0.14	0.1	0.08
$I_{s,k} / I_{s,k=1}$	1	0.04	0.02	0.008	0.006

- Amplitudes of current harmonics decrease with inverse of square of ordinal number k , because the leakage inductances **smooth** the shape of current (= they reduce the current harmonics !)



FOURIER sum of 25 current harmonics



Exact solution of dynamic machine equation with space vector theory

Additional machine losses at inverter-supply

- Additional cage losses:

Current displacement: AC deep bar resistance increases by ratio $k_{Rk} \cong h_{bar} / d_{E,k}$ with **penetration depth** (conductivity κ , permeability μ of rotor bar conductor)

$$d_{E,k} = 1 / \sqrt{\mu \cdot \kappa \cdot \pi \cdot f_{rk}} \approx 1 / \sqrt{\mu \cdot \kappa \cdot \pi \cdot |k| \cdot f_s} \quad .$$

Losses in bar conductors for k^{th} harmonic of voltage/current:

$$P_{ad,r,inv,k} = Q_r \cdot R_{r\sim} \cdot I_{r,k}^2 = Q_r \cdot k_{Rk} \cdot R_{r=} \cdot I_{r,k}^2 \cong Q_r \cdot k_{Rk} \cdot R_{r=} \cdot \frac{U_{s,k}^2}{(|k|\omega_s(L_{s\sigma} + L'_{r\sigma}))^2}$$

$$P_{ad,r,inv,k} \sim \sqrt{|k|} \cdot U_{s,k}^2 / |k|^2$$

- **Additional “iron losses”**: Rotor surface eddy current losses; losses in the end shields, ...
- **Additional inter-bar current losses**: rather small, as only field fundamental waves $\nu = 1$ are of considerable amplitude for $k \neq 1$. But field waves $\nu = 1$ do not produce much inter-bar currents in skewed cages.



Influence of rotor slot shape on additional cage losses AT LOW SWITCHING FREQUENCIES $f_T =$ HIGH POWER MOTORS

Example: $f_{sN} = 50$ Hz, Model motor 15 kW for investigating losses in high-power motors, synchronous switching, $f_T = 750$ Hz ($f_T/f_s = 15$):

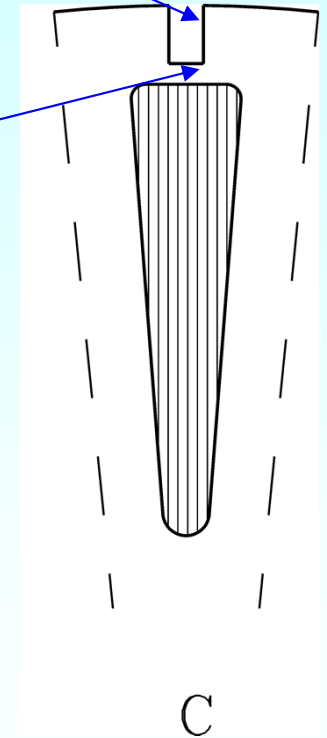
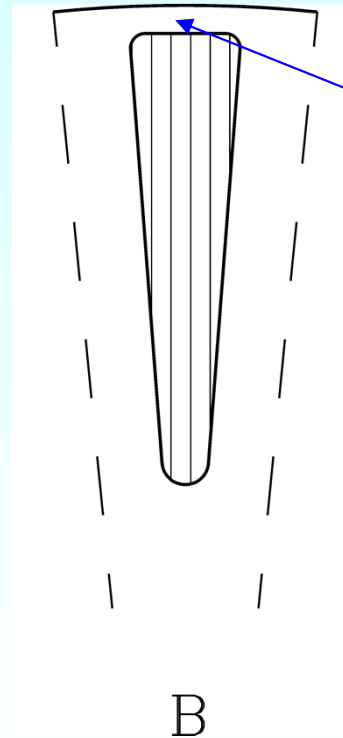
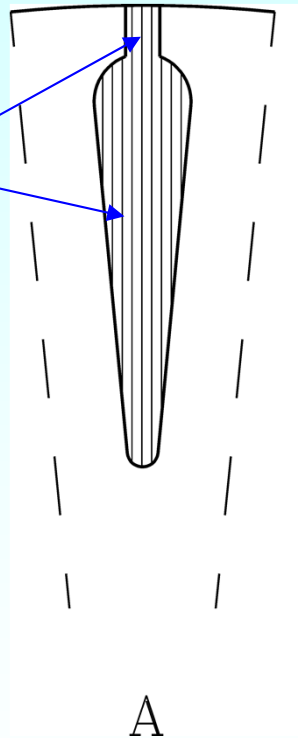
Additional cage losses: numerically determined:

Slot shape A: 190 W, slot shape C: 60 W.

- Slit gives independence of leakage inductance of bridge saturation

- surface eddy currents
- current displacement

- Closed bridge increases leakage inductance = reduction of harmonic currents



Source:
Arkkio, A.; ICEM, 1992

„not so good“

„good“

„better“

Increase of switching frequency to decrease add. losses

Example:

- 2-pole motor, 3 kW, 380 V Y; voltage source inverter 8.3 kVA, asynchronous switching ($f_T = \text{const.}$) with rating 8.3 kVA, 400 V.
- Motor is operated at $f_s = 50$ Hz, slip $s = 4.5\%$ at 10 Nm, 3 kW.
- Motor and inverter efficiency **were measured by directly** measuring input and output power both of motor and inverter for different inverter switching frequencies.

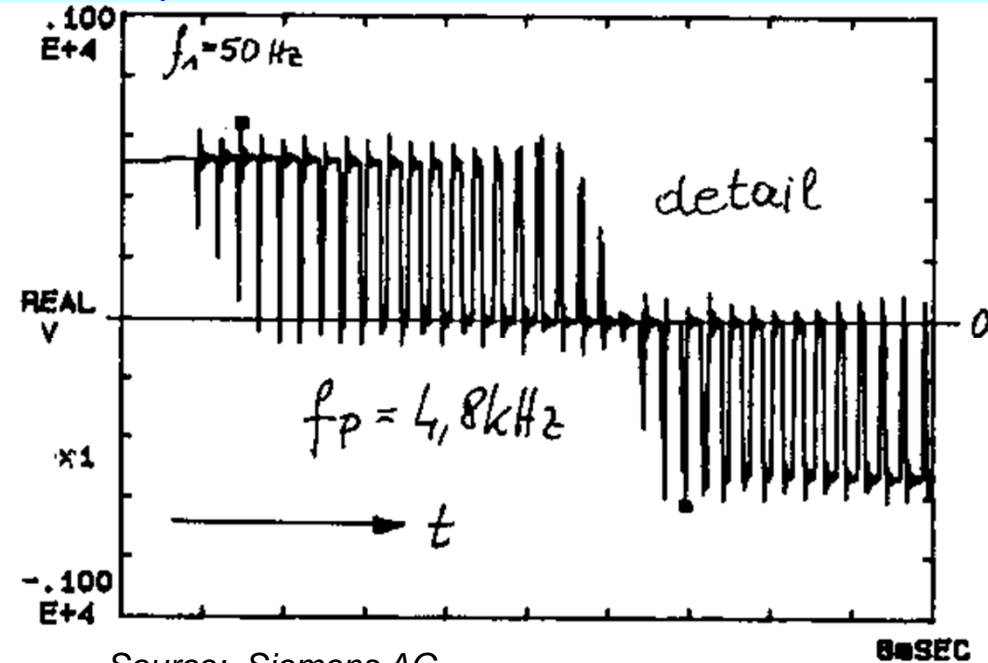
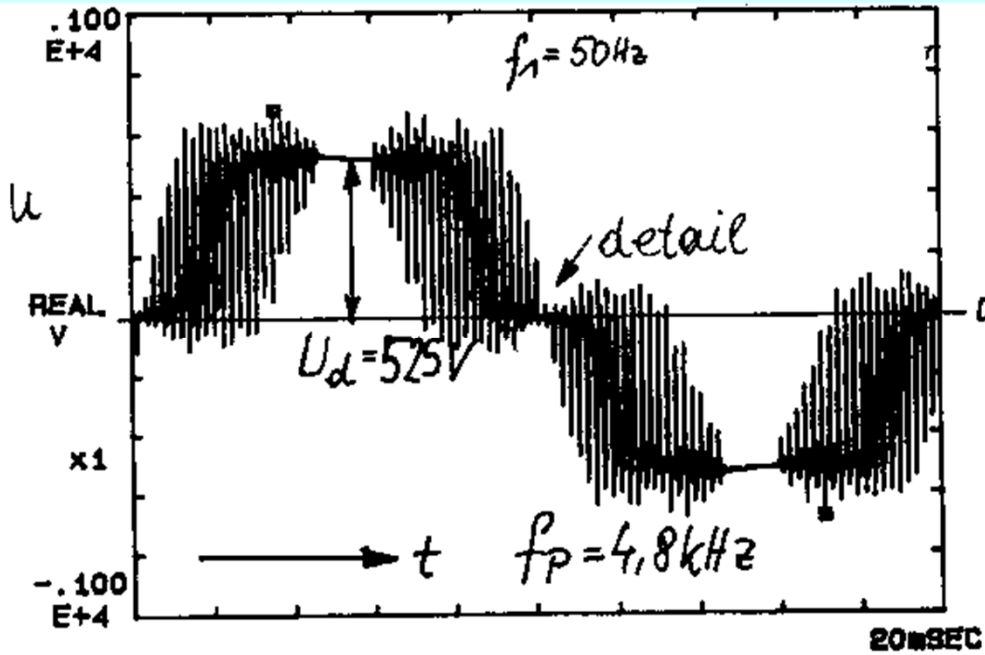
	<i>grid operation</i>	<i>inverter operation</i>		
f_s / Hz	50	50	50	50
f_T / Hz	-	2 400	4 800	9 600
$f_p = 2f_T / \text{kHz}$	-	4.8	9.6	19.2
Efficiency motor	81.9 %	81.3 %	81.4 %	81.4 %
Efficiency inverter	-	96.9 %	96.8 %	95.9 %
Overall efficiency	81.9 %	78.8 %	78.8 %	78.1 %

Facit:

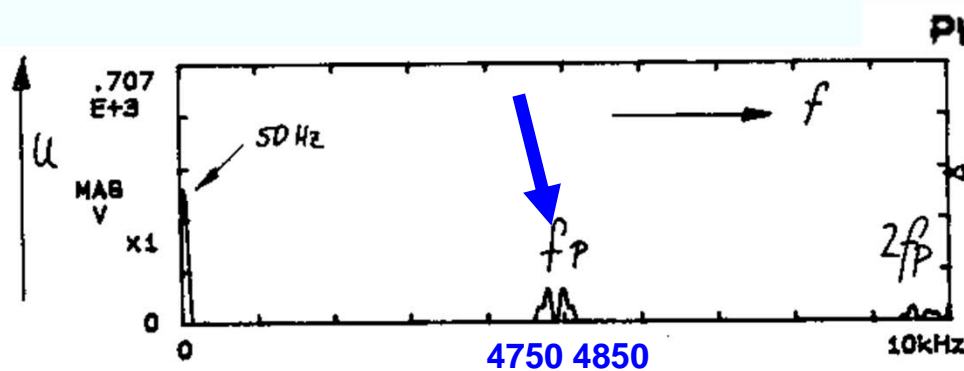
At $f_p = 9.6$ kHz the motor efficiency is higher (motor heating is lower), and the overall efficiency is the same as at 4.8 kHz. At 19.2 kHz the current ripple reduction in the motor is already negligible, but inverter switching losses increase considerably.

Measured PWM voltage

Measured *Fourier* spectrum of line-to-line voltage, $f_T = 2.4$ kHz, $f_p = 2f_T = 4.8$ kHz, 2-pole induction motor, 3 kW, load operation, $U_{LL,rms} = 403$ V



Source: Siemens AG

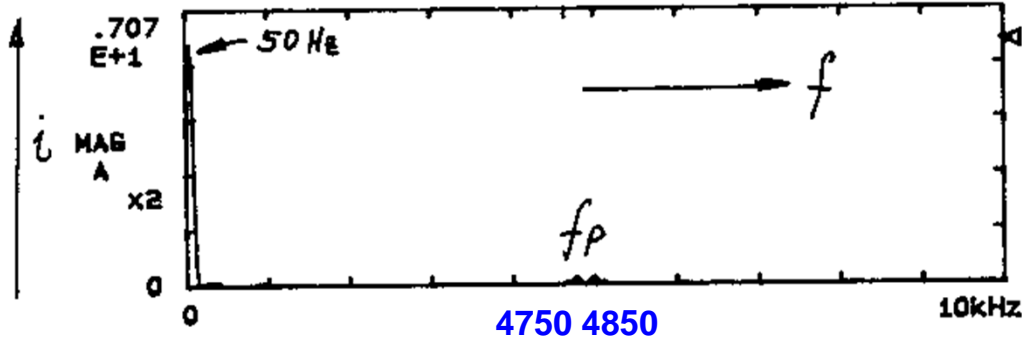
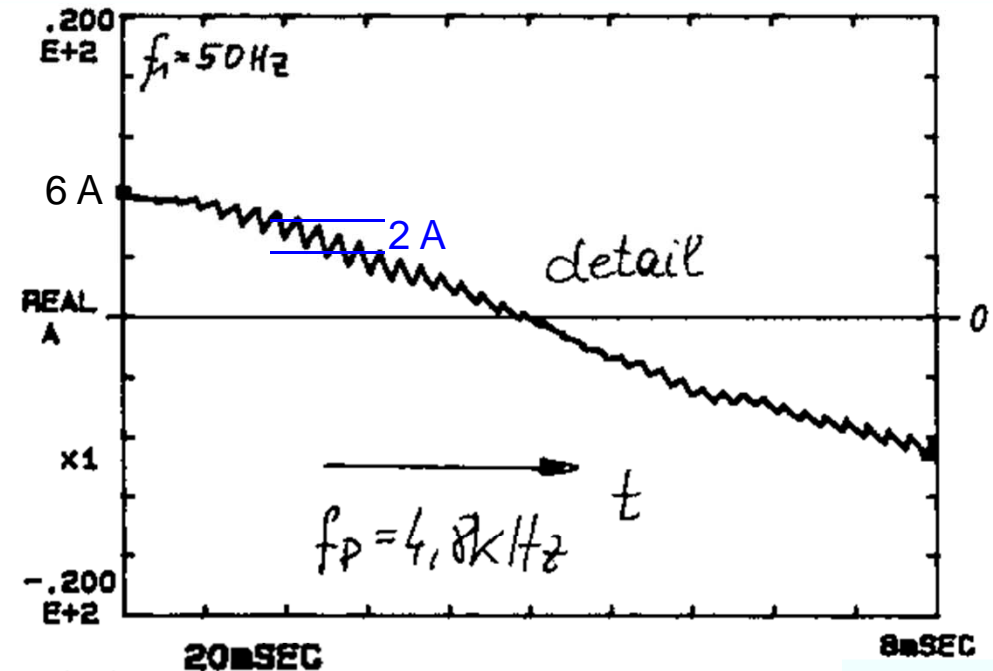
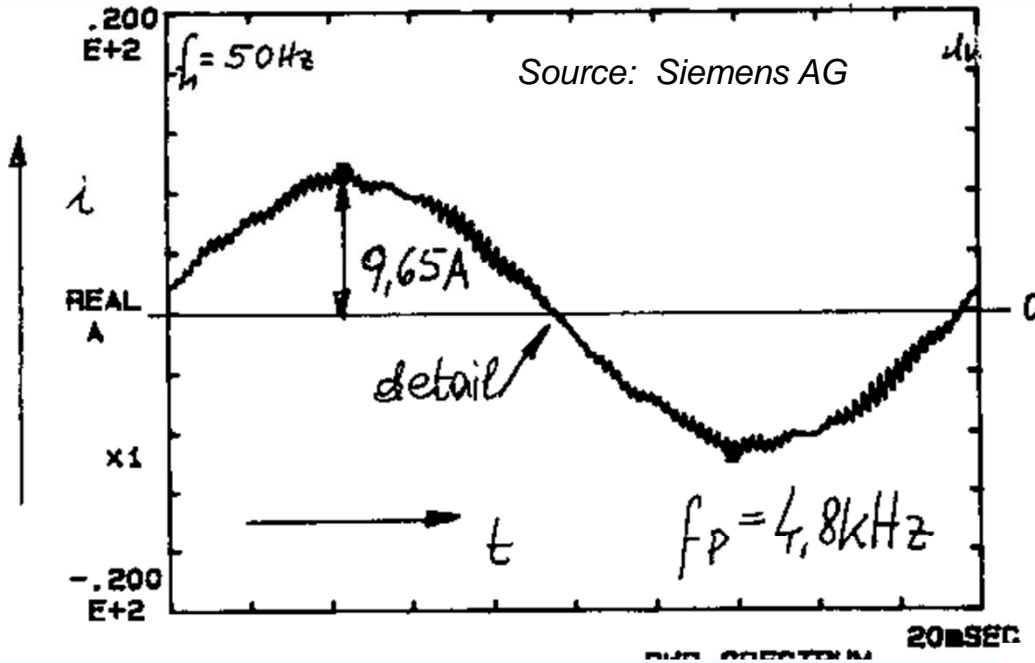


PWA SPECTRUM

1	50Hz	.372E+3 V
2	4975	.919E+2 ← 4850 Hz
3	4775	.895E+2 ← 4750 Hz
4	5075	.431E+2
5	9525	.386E+2
6	9725	.248E+2
7	9825	.219E+2
8	275	.293E+1

Measured motor current at PWM feeding

Measured *Fourier* spectrum of phase motor current, $f_T = 2.4$ kHz, $f_p = 2f_T = 4.8$ kHz, 2-pole induction motor, 3 kW, load operation, **r.m.s. current 6.25 A**



PWR SPECTRUM

1	50Hz	.620E+1	A
2	4775	.182E+0	← 4750 Hz
3	4975	.183E+0	← 4850 Hz
4	350	.113E+0	
5	250	.913E-1	
6	925	.849E-1	
7	1125	.515E-1	
8	650	.281E-1	
9	9550	.352E-1	← 36 mA
10	9750	.267E-1	←

Determination of harmonic stator/rotor currents

Example:

Measured *Fourier* spectrum of line-to-line voltage & phase motor current, $f_T = 2.4\text{kHz}$

		$U_{LL,k}$	$I_{s,k}$	$I_{s,k} / I_{s,k=1}$
f_s	50 Hz	372 V	6.2 A	100 %
$2f_T - f_s$	4750 Hz	89.5 V	0.18 A	2.9 %
$2f_T + f_s$	4850 Hz	91.3 V	0.18 A	2.9 %
$4f_T - f_s$	9550 Hz	38.6 V	0.035 A	0.6 %
$4f_T + f_s$	9650 Hz	24.8 V	0.027 A	0.4 %

-Time harmonic current:
$$\text{e.g. at } 9550 \text{ Hz: } I_{sk} = \frac{U_{LL,k} / \sqrt{3}}{\omega_{sk} \cdot (L_{s\sigma} + L'_{r\sigma})} = \frac{38.6 / \sqrt{3}}{2\pi \cdot 9550 \cdot 0.00961} = \underline{\underline{38.6 \text{ mA}}} \text{ (measured: 35 mA)}$$

- Peak-to-peak current ripple: Two phases in series: $2L_\sigma$ active. $L_\sigma = L_{s\sigma} + L'_{r\sigma}$

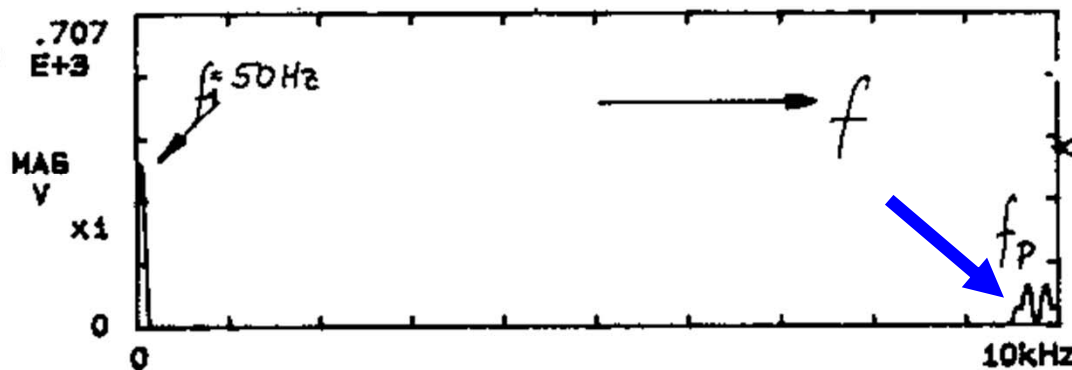
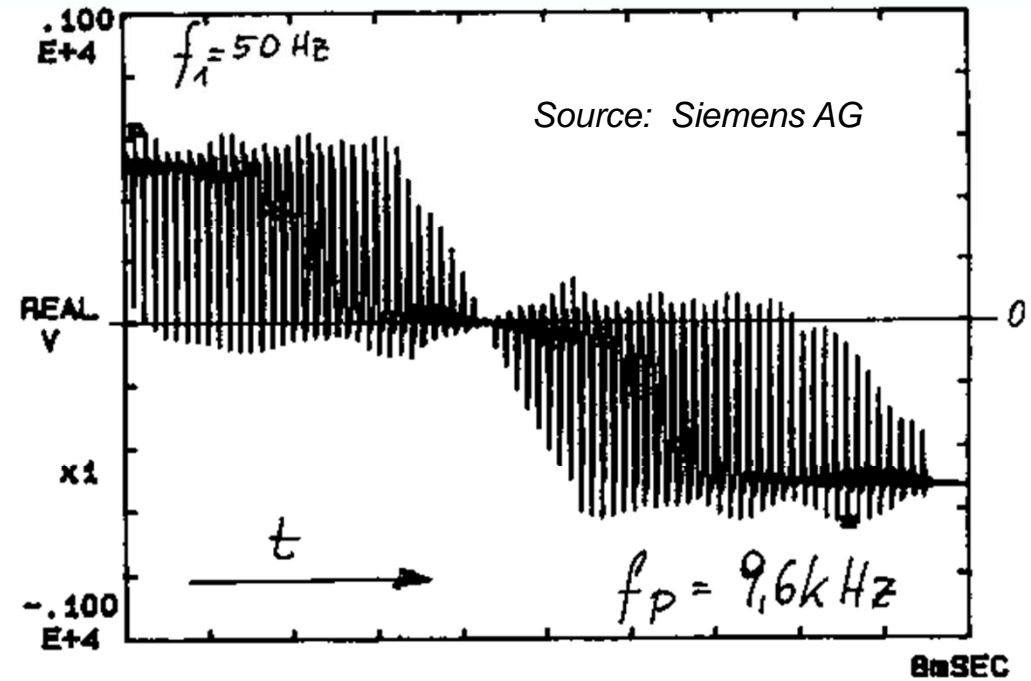
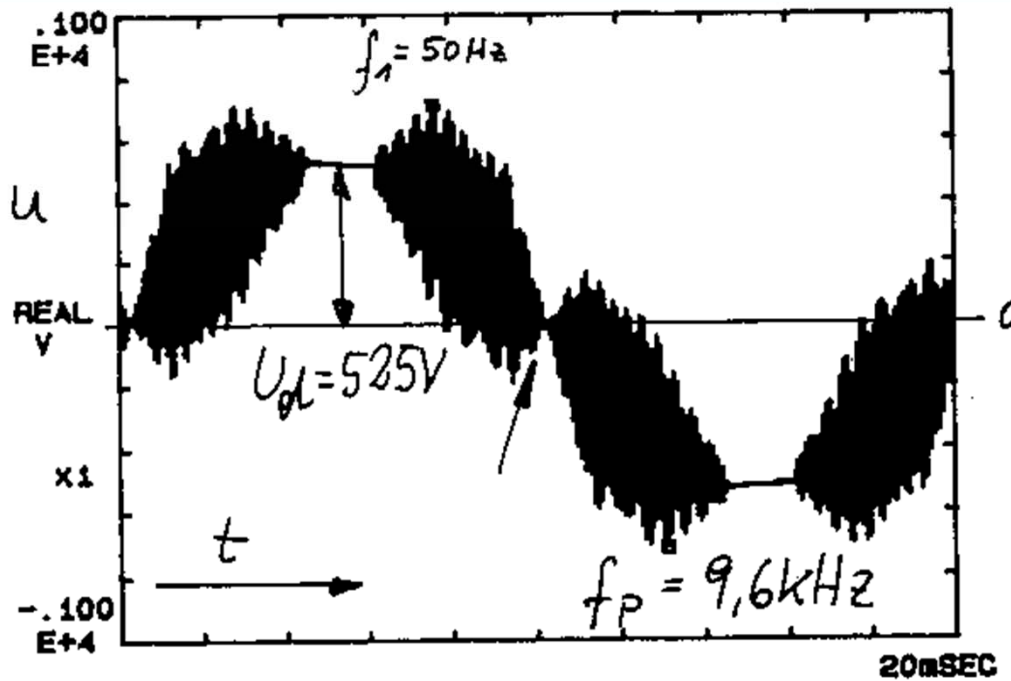
$$u = L \cdot di / dt \Rightarrow U_d = 2L_\sigma \cdot \Delta i / \Delta t, \quad \Delta t \cong T_p / 2 = 1 / (2f_p):$$

$$\Delta i = \frac{U_d}{4L_\sigma f_p} = \frac{525}{4 \cdot 0.00961 \cdot 4800} = \underline{\underline{2.8 \text{ A}}}$$

$$2.8 \text{ A} / (2 \cdot \sqrt{2}) \approx 1 \text{ A} \approx \sum_k |I_{-k}|$$

Measured PWM voltage at increased switching frequency

Measured *Fourier* spectrum of line-to-line voltage, $f_T = 4.8 \text{ kHz}$, $f_p = 2f_T = 9.6 \text{ kHz}$, 2-pole induction motor, 3 kW, load operation, $U_{LL,rms} = 401 \text{ V}$

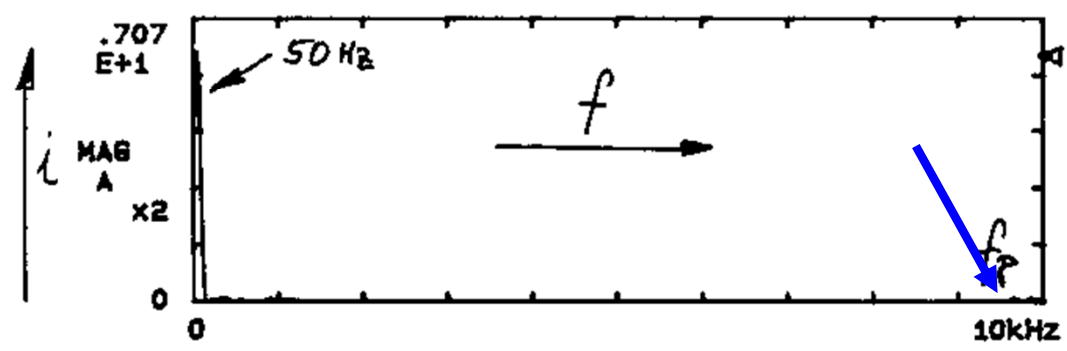
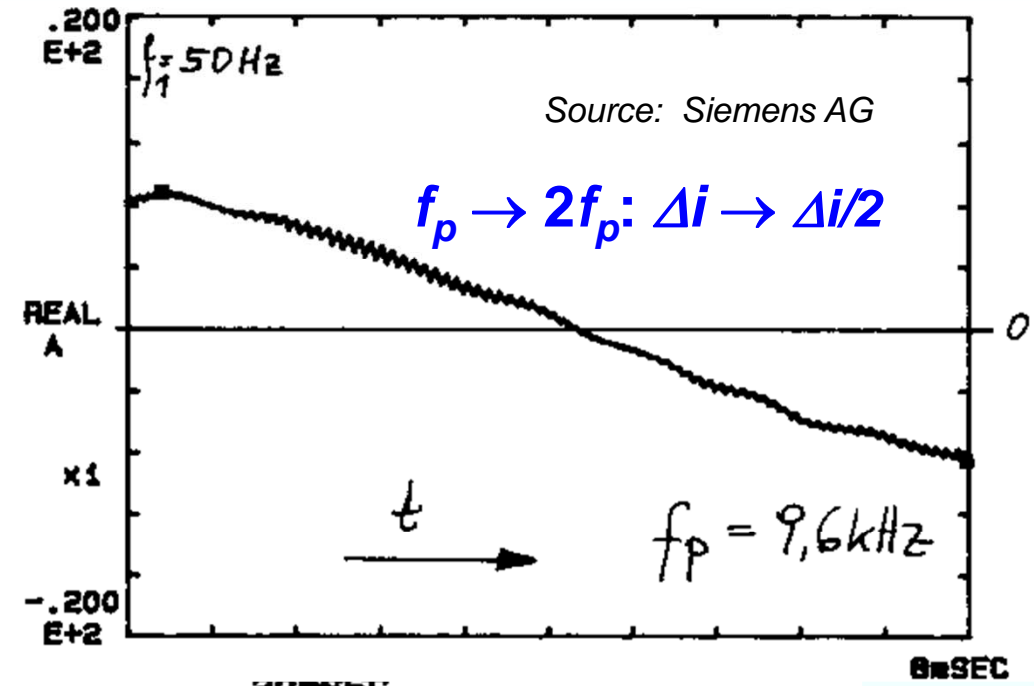
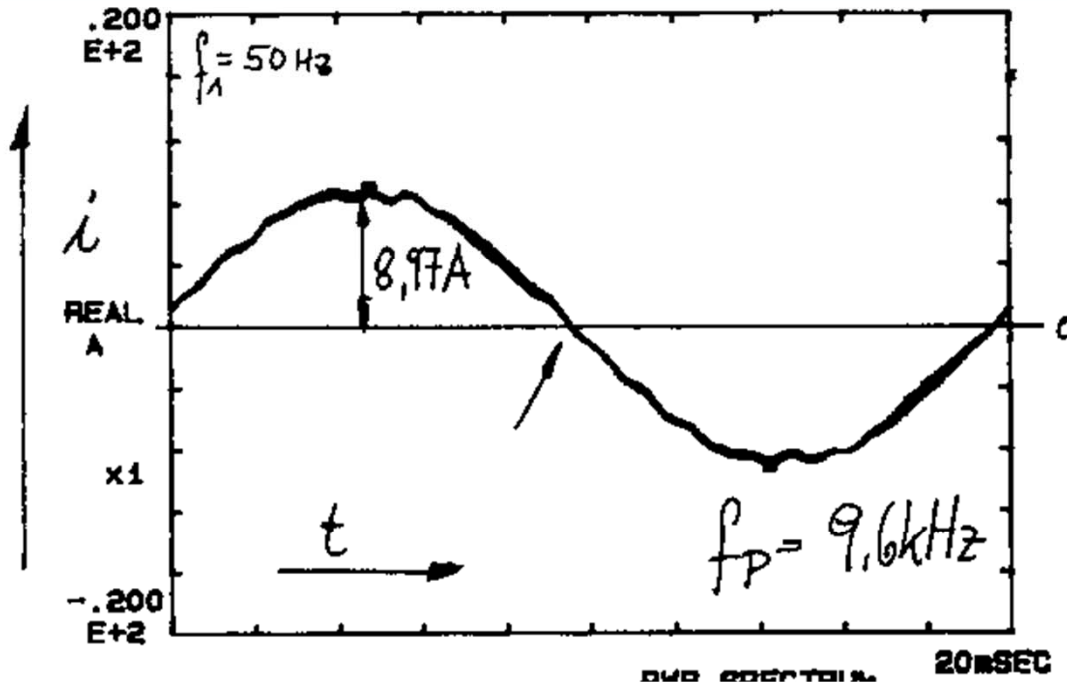


SPECTRUM

1	50Hz	.372E+3	V
2	9675	.893E+2	← 9650 Hz
3	9675	.899E+2	
4	9975	.421E+2	← 9550 Hz
5	9575	.419E+2	
6	275	.258E+1	
7	325	.227E+1	
8	675	.222E+1	
9	9275	.243E+1	

Measured motor current at increased switching frequency

Measured *Fourier* spectrum of phase motor current, $f_T = 4.8$ kHz, $f_p = 2f_T = 9.6$ kHz, 2-pole induction motor, 3 kW, load operation, **r.m.s. current 6.27 A**

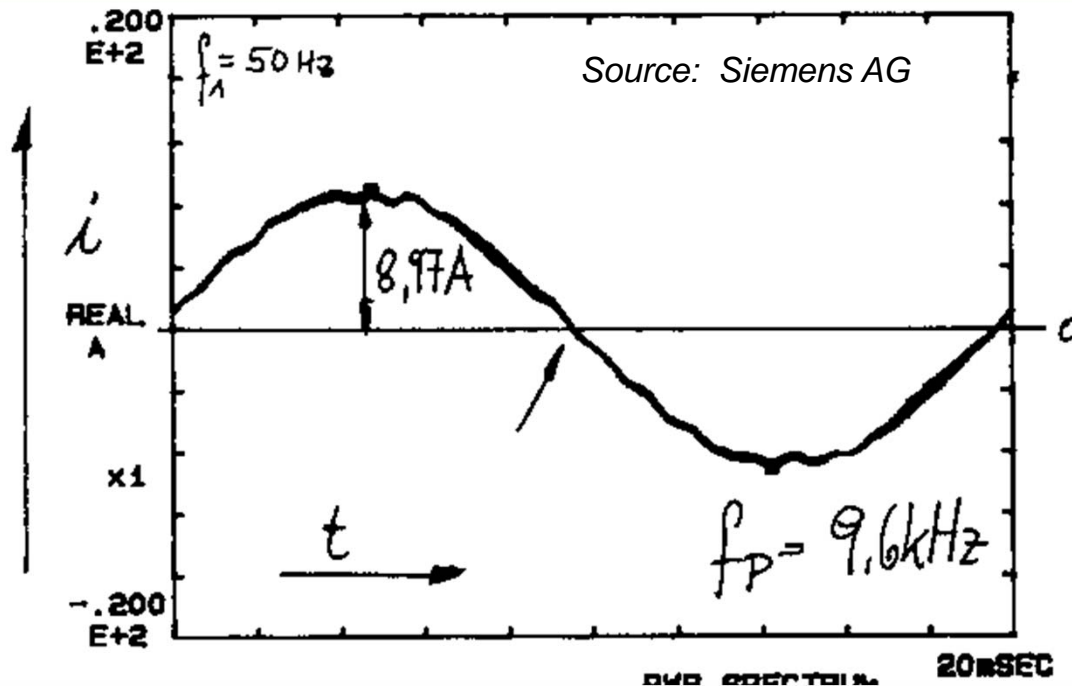


SPECTRUM	2UMSEC	
1	50Hz	.625E+1 A
2	375	.915E-1
3	900	.912E-1
4	9675	.101E+0 ← 9650 Hz
5	9875	.102E+0 ←
6	1125	.495E-1
7	9975	.481E-1 ←
8	675	.292E-1
9		

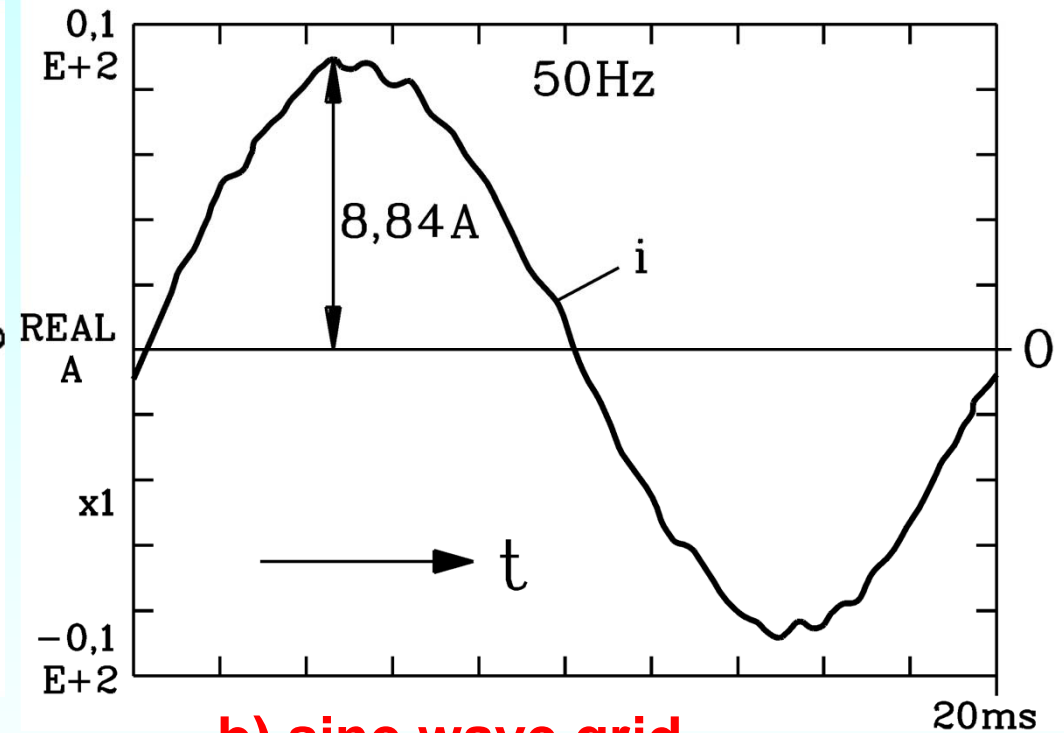


Measured motor current at a) PWM and b) grid operation

Measured *Fourier* spectrum of phase motor current, $f_T = 4.8$ kHz, $f_p = 2f_T = 9.6$ kHz, 2-pole induction motor, 3 kW, load operation, **r.m.s. current 6.27 A**



a) PWM



b) sine wave grid

- **Nearly no** difference between current wave form at PWM with high switching frequency and sine wave voltage operation.
- **Harmonic content** in the stator current is caused mainly by rotor slot harmonics of the air-gap field, excited by the fundamental rotor current.

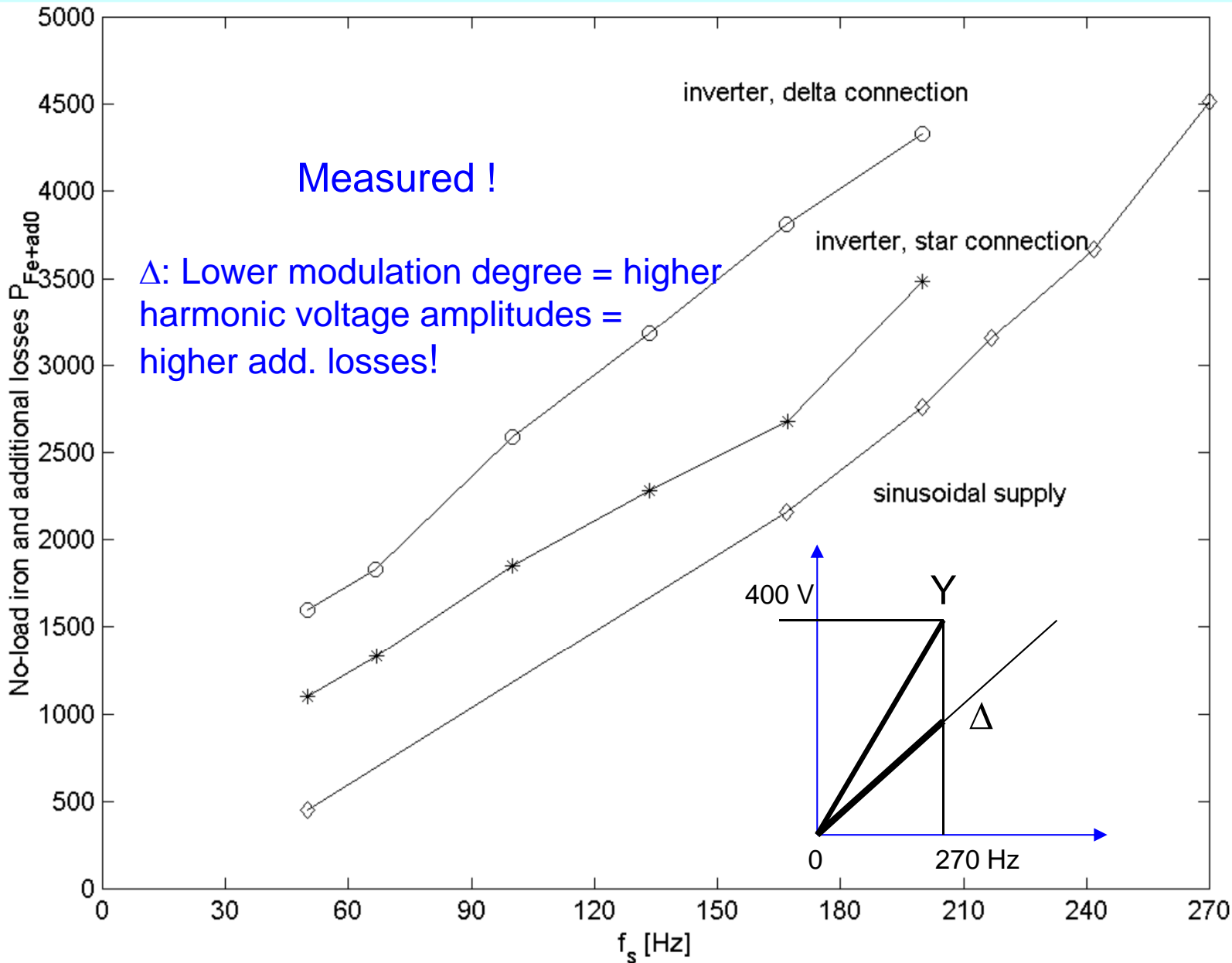
No-load iron and additional losses at sinus and inverter supply

270 kW, 400 V, 2-poles,
high-speed induction
machine,
max. 16000/min

Comparison of no-load
iron and additional losses

- a) Sinus supply
- b) IGBT-PWM-Inverter-
supply, 4 kHz,
star connection Y,
- c) delta connection D.

Dependence of stator
fundamental frequency f_s .
During measurements air
gap flux density had been
maintained constant.



Measured !

Δ : Lower modulation degree = higher
harmonic voltage amplitudes =
higher add. losses!

Inverter-induced torque ripple

- Fundamental air gap field amplitudes $B_{\delta sk, v=1}$ of stator harmonic currents I_{sk} produce with rotor harmonic currents I_{rk} tangential *Lorentz*-forces, and therefore additional torque components.

- Stator field $B_{\delta sk=1, v=1}$, excited by fundamental current $I_{s, k=1}$, generates with rotor harmonic current I_{rk} of DIFFERENT ordinal number k a **pulsating** torque $M_{e, 1k}$, which is proportional to product $M_{e, 1k} \sim B_{\delta sk=1, v=1} \cdot I_{rk}$ or due to $B_{\delta sk=1, v=1} \sim I_{sk=1}$ it is $M_{e, 1k} \sim I_{s1} \cdot I_{rk}$. **Pulsating frequency:** $f_{1k} = |f_s - f_{sk}|$

- As $f_{1k} = |1 - k|f_s = 6|g|f_s$, the pulsating torque occurs with multiples of six time stator fundamental frequency.
- Each two harmonics contribute with their torque amplitudes to one resulting pulsating torque with the sum of both torque amplitudes:

Example:

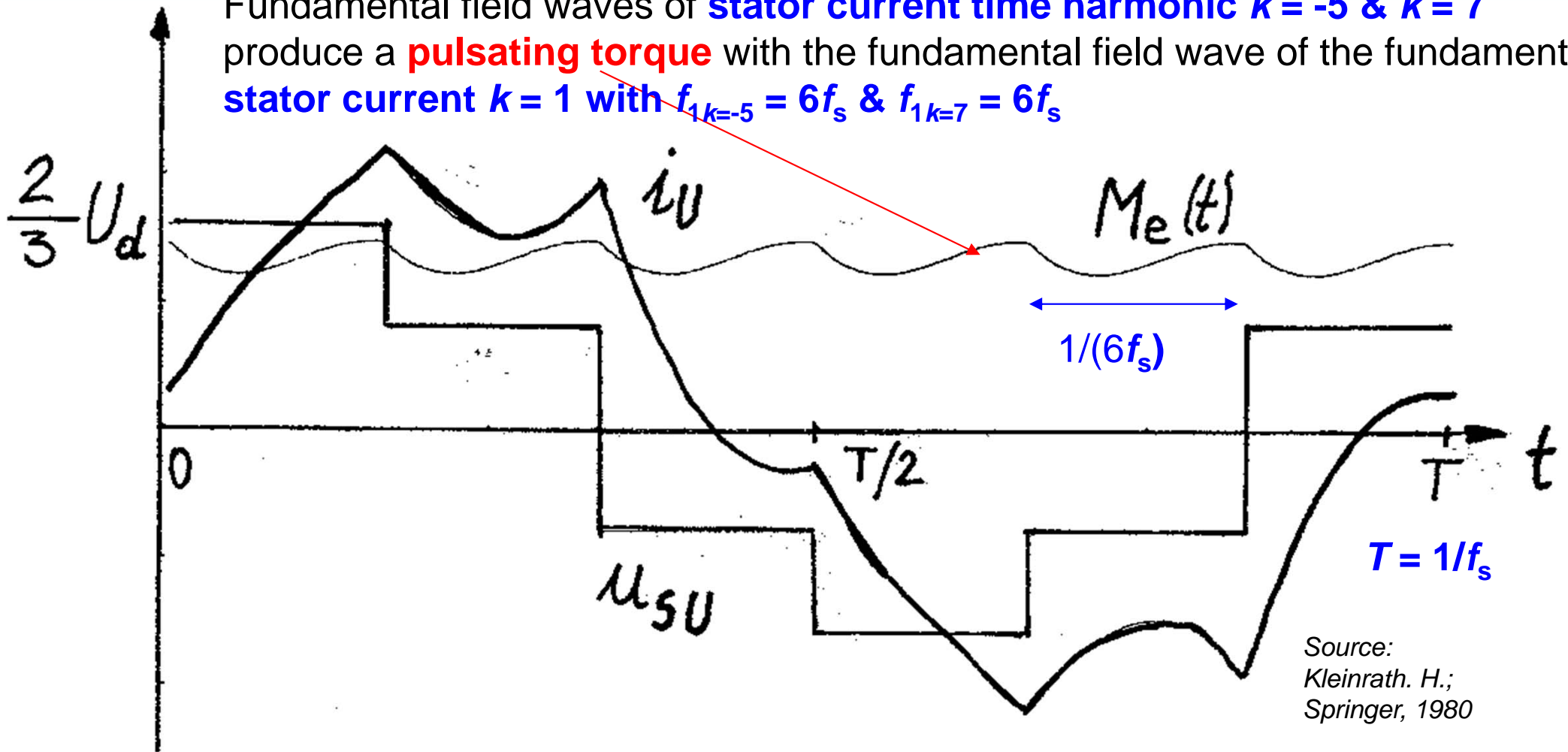
$k = -5$ and $k = 7$: $\hat{M}_{e, 1, -5}$, $\hat{M}_{e, 1, 7}$, frequency $6f_s$

resulting amplitude $\hat{M}_{e, 6f_s} = \hat{M}_{e, 1, -5} + \hat{M}_{e, 1, 7}$.



Torque ripple amplitude at six-step operation

Fundamental field waves of **stator current time harmonic $k = -5$ & $k = 7$** produce a **pulsating torque** with the fundamental field wave of the fundamental stator current $k = 1$ with $f_{1k=-5} = 6f_s$ & $f_{1k=7} = 6f_s$



Source:
Kleinrath. H.;
Springer, 1980

Ripple frequency = 6-times fundamental frequency and multiples

Air-gap torque ripple amplitude

$$M_{e,1k} = \frac{p \tau_p \cdot Q_r \cdot \hat{I}_{rk} \cdot B_{\delta s} \cdot l_{Fe}}{2\pi} \cdot \sin((1-k)\omega_s t) \quad B_{\delta s} = B_{\delta s, k=1, \nu=1}$$

Example:

8-pole induction motor, 440 V Y, 60 Hz, 2.6 kW, 5.6 A, 28.4 Nm, 860/min, inverter supply at $f_s = 50$ Hz, $U_d = 525$ V, PWM, switching frequency $f_T = 2.4$ kHz

Motor data: $m_s = 3$, $Q_s/Q_r = 48/44$, $l_{Fe} = 80$ mm, $L_\sigma = 19.6$ mH, $k_{ws} = 0.933$, $N_s = 344$, stator field fundamental: $B_{\delta s} = 1$ T

$$\hat{I}_{rk} = -\frac{m_s N_s k_{ws}}{Q_r / 2} \cdot \frac{\hat{U}_{s,k}}{|k| \omega_s L_\sigma}$$

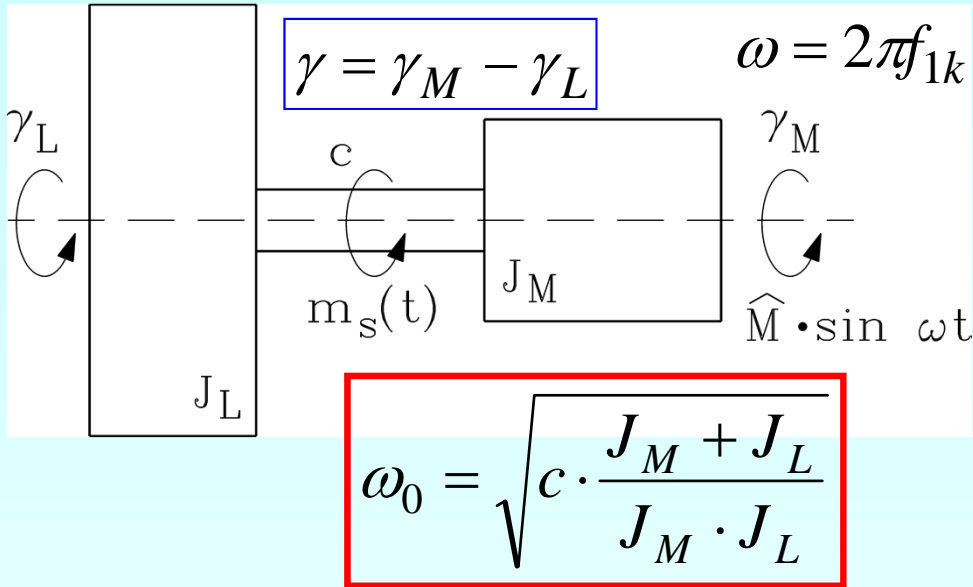
$$2f_T/f_s \pm 1 = 95, 97: k = -95, 97$$

$$f_{1k} = |f_s - f_{sk}| = |1 - k| f_s = 96 f_s = 4.8 \text{ kHz}$$

Air gap torque ripple: $1.68/28.4 = 5.9\%$
 Shaft torque ripple: 0.0015 Nm (= 0.005%)
 due to rotor inertia and elastic coupling

$ k $	f_k	$\hat{U}_{s,k}$	\hat{I}_{rk}	$\hat{M}_{e,1k}$	$\hat{M}_{e,6 g f_s}$	f_{1k}
-	Hz	V	A	Nm	Nm	Hz
95	4750	73.1	5.5	0.85		
97	4850	74.2	5.4	0.83		
					1.68	4800

Shaft-torque much smoother than air-gap torque



Rotor of motor coupled to rotating load via an elastic coupling

- coupling stiffness c
- inertia of motor and load J_M, J_L

Resonance frequency f_0 :

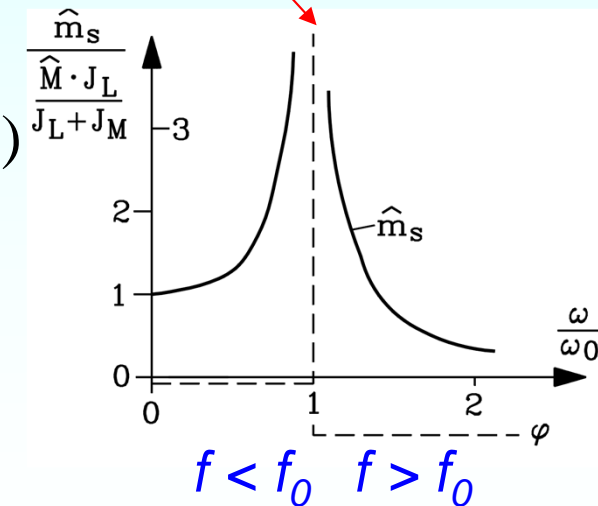
big ... small motors: 20 Hz ... 200 Hz

Pulsating shaft torque: $m_s(t) = c \cdot \gamma(t) = \frac{\hat{M}}{J_M} \cdot \frac{c}{\omega_o^2 - \omega^2} \cdot \sin(\omega t)$

Low exciting frequency $f < f_0$: $m_s(t) \cong \hat{M} \cdot \frac{J_L}{J_M + J_L} \cdot \sin(\omega t)$

High exciting frequency $f > f_0$: $m_s(t) \cong -\frac{\hat{M}}{J_M} \cdot \frac{c}{\omega^2} \cdot \sin(\omega t)$

Facit: Switching frequency torque ripple smoothed strongly by rotor inertia and elastic coupling above f_0 !



Air-gap torque ripple amplitude

Shaft torque ripple is **below** torsion resonance f_0 determined by ratio of load versus motor inertia, **above** resonance by the inverse square of pulsation frequency

$$f_{1k} < f_0 : \hat{M}_s \cong \frac{\hat{M}_{e,6|g|f_s} \cdot J_L}{J_L + J_M}$$

$$f_{1k} > f_0 : \hat{M}_s \cong \frac{\hat{M}_{e,6|g|f_s} \cdot c}{J_M \cdot (2\pi f_{1k})^2}$$

Example:

$$f_0 = 200 \text{ Hz}, f_s = 10 \text{ Hz}, J_L = J_M$$

$$\text{a) } f_{1k} = 6f_s = 60 \text{ Hz} < 200 \text{ Hz}$$

$$\text{b) } f_{1k} = 2f_T = 4.8 \text{ kHz} > 200 \text{ Hz.}$$

Torque ripple:

- in air gap: 3.3%

5.9%

- at the shaft: 1.7%

0.005%

Although $6f_s$ -torque ripple in the air gap is lower, the shaft torque ripple with $6f_s$ is dominating over high harmonic torque components.

Due to speed and frequency variation the torsion resonance might be hit.

Measured shaft torque ripple: Low n , high J_L

Example: Low speed 20/min

Induction motor: 2 pole, 750 W, 2850/min, 2.51 Nm, 400 V D, 50 Hz, 1.6 A

Voltage-source IGBT Inverter: 1500 VA, 2.2 A, 400 V

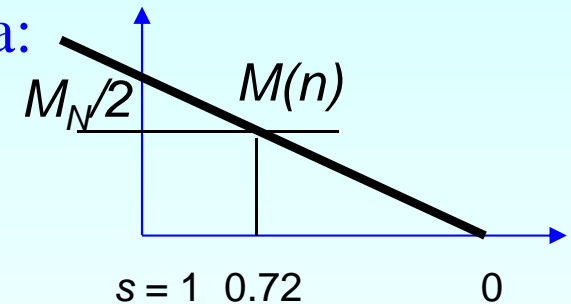
Motor operated at $f_s = 1.2$ Hz, $n = 20$ /min, $s = 0.72$, $M = 1.24$ Nm = 50% rated torque

a) PWM, asynchronous switching: $k = 1 + 6g = 1, -5, 7, -11, 13, \dots$ $g = 0, \pm 1, \pm 2, \dots$

b) PWM voltage output pattern is not symmetrical to abscissa:

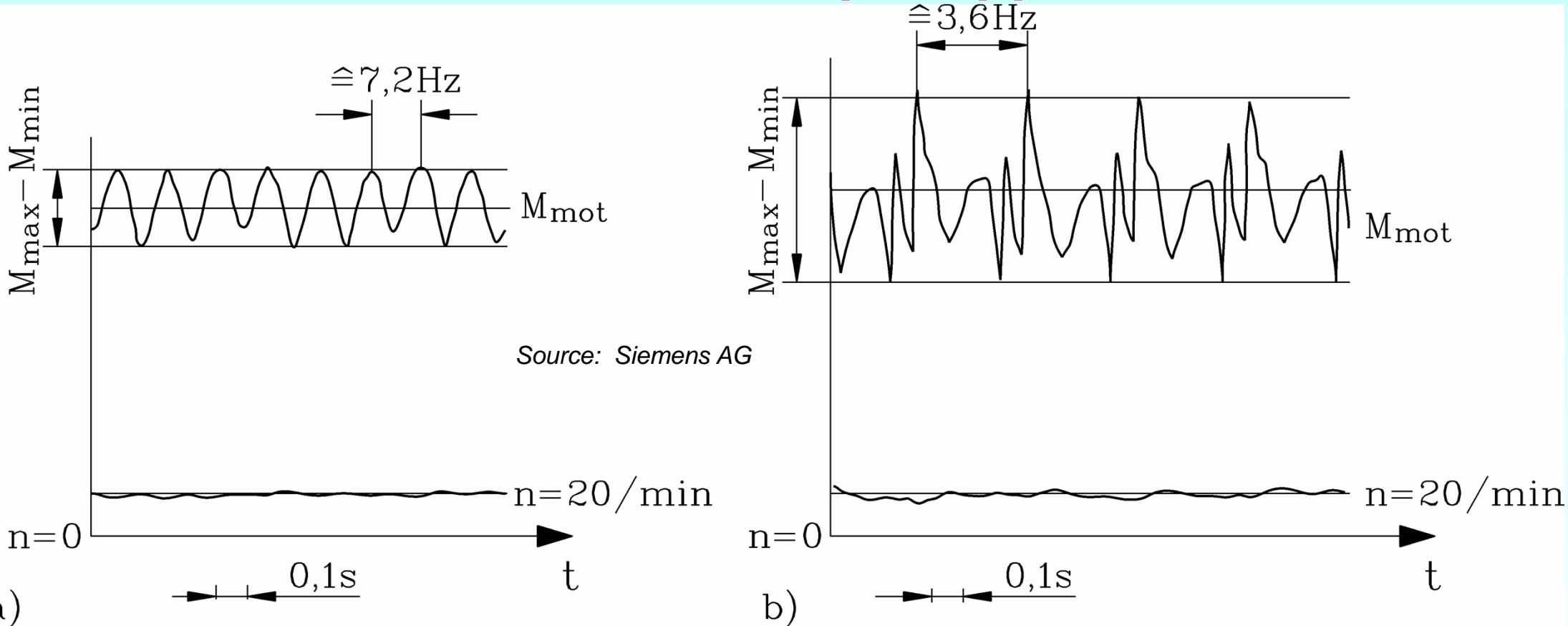
Voltage harmonics with even ordinal numbers occur:

$k = 1 + 3g = 1, -2, 4, -5, 7, -8, 10, -11, 13, \dots$ $g = 0, \pm 1, \pm 2, \dots$



	a) symmetrical PWM	b) asymmetrical PWM
Lowest torque ripple frequency	$f_{1k} = 6 g f_s = 6f_s =$ $= 6 \cdot 1.2 = 7.2 \text{ Hz}$	$f_{1k} = 3 g f_s = 3f_s =$ $= 3 \cdot 1.2 = 3.6 \text{ Hz}$
Measured torque ripple \hat{w}_M	14.4%	35.0%
Torque ripple amplitude	0.18 Nm	0.43 Nm

Measured torque ripple



	a) symmetrical PWM	b) asymmetrical PWM
Lowest torque ripple frequency	$f_{1k} = 6 g f_s = 6f_s =$ $= 6 \cdot 1.2 = 7.2\text{Hz}$	$f_{1k} = 3 g f_s = 3f_s =$ $= 3 \cdot 1.2 = 3.6\text{Hz}$
Torque ripple amplitude	0.18 Nm	0.43 Nm



Inverter-induced acoustic noise

- In addition to the magnetically excited acoustic noise at sinus voltage supply, additional air gap waves $\nu = 1$ of the current harmonics I_{sk} will add to acoustic noise with new tonal frequencies, **mainly with inverter pulse frequency $f_p = 2f_T$** .

Stator fundamental field waves ($\nu = 1$):

a) excited by magnetizing current $\underline{I}_m = \underline{I}_s + \underline{I}'_r$ with stator frequency f_s :

$$B_{\delta sk=1, \nu=1}(x_s, t) = B_{\delta s} \cdot \cos\left(\frac{\pi x_s}{\tau_p} - 2\pi f_s t\right) = B_{\delta s} \cdot \cos\left(\frac{2p\pi x_s}{2p\tau_p} - 2\pi f_s t\right) = B_{\delta s} \cdot \cos \alpha$$

b) excited by magnetizing current $\underline{I}_{mk} = \underline{I}_{sk} + \underline{I}'_{rk}$ with stator harmonic frequency f_{sk} :

$$B_{\delta sk, \nu=1}(x_s, t) = B_{\delta sk} \cdot \cos\left(\frac{2p\pi x_s}{2p\tau_p} - 2\pi \cdot k \cdot f_s t\right) = B_{\delta sk} \cdot \cos \beta$$

$$\text{Magnetic pull: } f_n(x_s, t) = \frac{B^2(x_s, t)}{2\mu_0} \sim \left(\sum_{k=1}^{\infty} B_{\delta sk}\right)^2 \Rightarrow f_{n,1k} \sim \sum_{k, k'=1}^{\infty} B_{\delta sk}^2 + 2B_{\delta sk} B_{\delta sk'} \quad k \neq k'$$

Radial force density waves, causing oscillating pull on iron stack: $f_{n,1k} \sim \cos(\alpha \pm \beta)$

$$f_{n,1k}(x_s, t) = \frac{B_{\delta s} B_{\delta sk}}{2\mu_0} \cdot \cos\left(2r \cdot \frac{\pi x_s}{2p\tau_p} - 2\pi f_{Ton,k} t\right)$$

Vibration mode of inverter-induced acoustic noise

Example:

$$2p = 4, 2r = 0 \text{ or } 8.$$

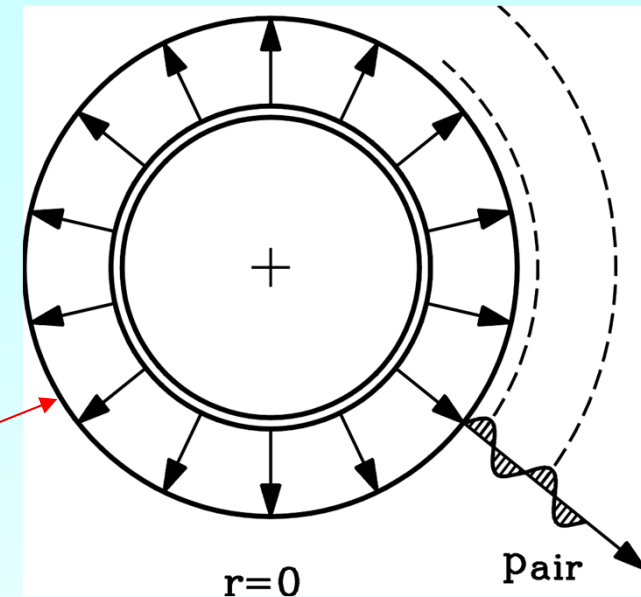
Tonal frequency $f_{Ton,k}$:

$$f_{Ton,k} = f_s \cdot |1 + k|$$

for $2r = 4p$

$$f_{Ton,k} = f_s \cdot |1 - k|$$

for $2r = 0$



Dominating current harmonic amplitudes at frequencies $f_{sk} = 2f_T \pm f_s$.

Dominating acoustic noise at

$$f_{Ton,k} = f_s \cdot |1 - k| = f_{sk} - f_s = 2f_T \quad \text{or} \quad f_{Ton,k} = 2f_T - 2f_s.$$

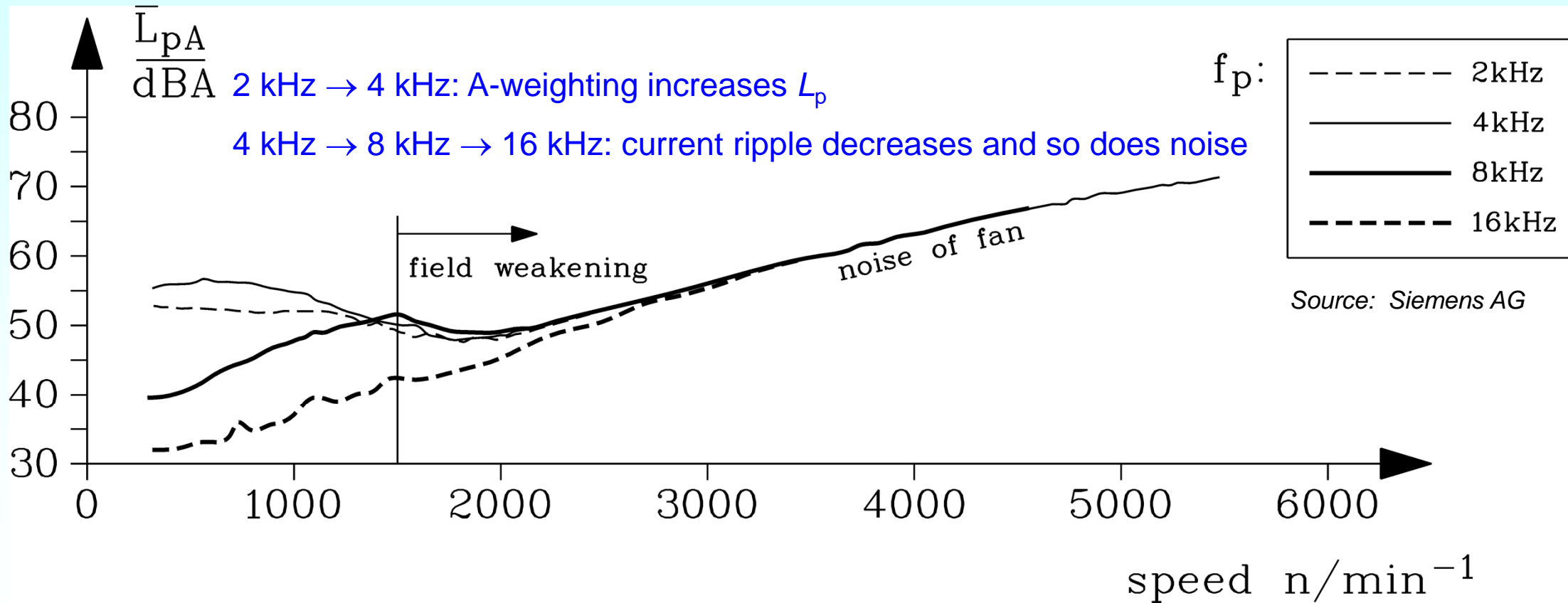
Inverter caused magnetic noise is usually excited with twice switching frequency ("pulse frequency"). Modal vibration is $r = 0$, so the sound is far reaching and well audible.

Influence of switching frequency on acoustic noise at inverter-operation

Measured A-weighted sound pressure level at 1 m distance:

250 W, PWM inverter-fed induction motor,

Varying switching frequency f_T and pulse frequency $f_p = 2f_T$.



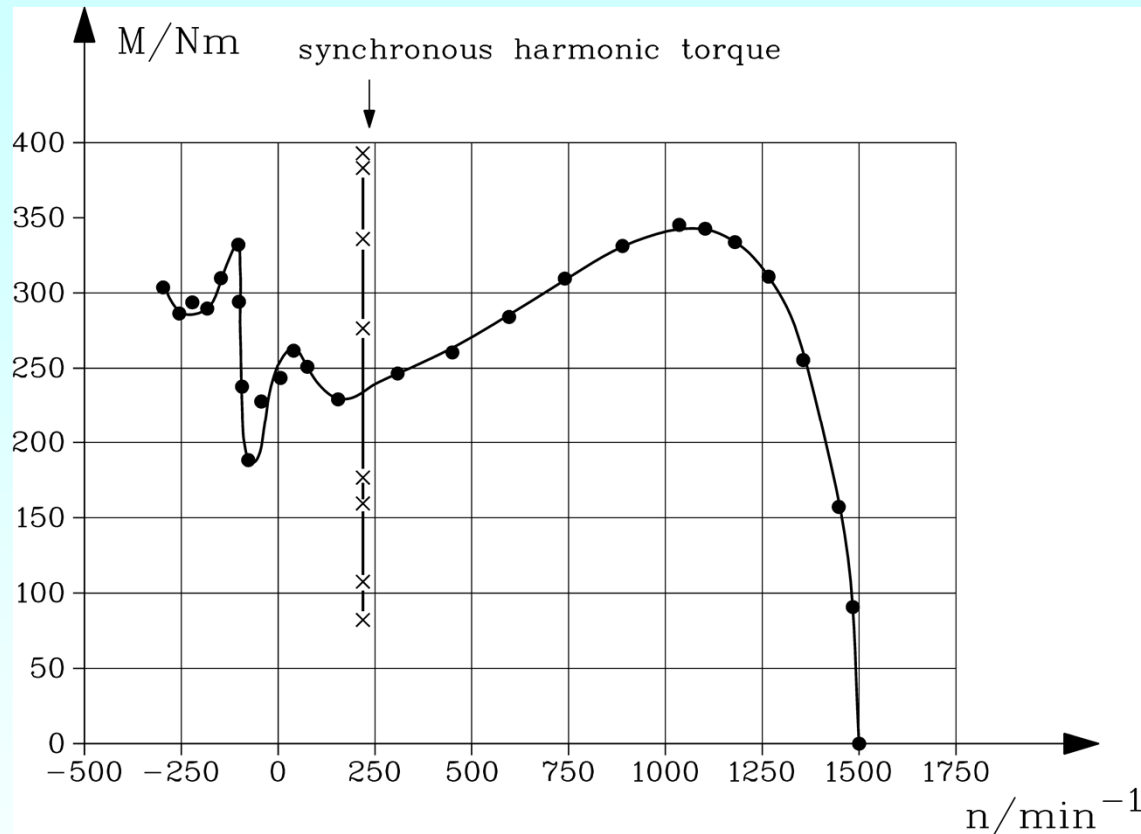
Influence of space harmonics at inverter-operation

- Asynchronous and synchronous harmonic torque occur at big slip: $s = 0.8 \dots 1.2$
- At low speed, full-load slip increases up to unity, so space harmonic torques are in the range of motor operation.
- **Motor current: ~ rated current (not – as during line-start – ~ 500% of I_N). So parasitic torque ~ I^2 components are negligible.**

Example: Unskewed 4-pole cage induction motor, 15 kW, 380 V, D, 50 Hz, 30 A, $Q_s/Q_r = 36 / 28$. Synchronous harmonic torque at slip 0.86: harmonics $\nu = -\mu = 13$, speed 215/min.

	<i>a) 50 Hz line operation</i>	<i>b) 1.5 Hz inverter operation</i>
Synchronous speed	1500/min	45/min
speed at rated torque 98 Nm	1460/min	5/min
slip at rated torque 98 Nm	2.6 %	88.9 %
rotor frequency at 98 Nm	1.3 Hz	1.3 Hz
current at slip 0.86 (synchronous harmonic torque)	550 % rated current	100% rated current
speed at synchronous torque	$(1-0.86)1500=215/\text{min}$	$(1-0.86)45=6.3 /\text{min}$
Synchronous torque amplitude	150 Nm	$150 \cdot (1/5.5)^2 = 5 \text{ Nm}$

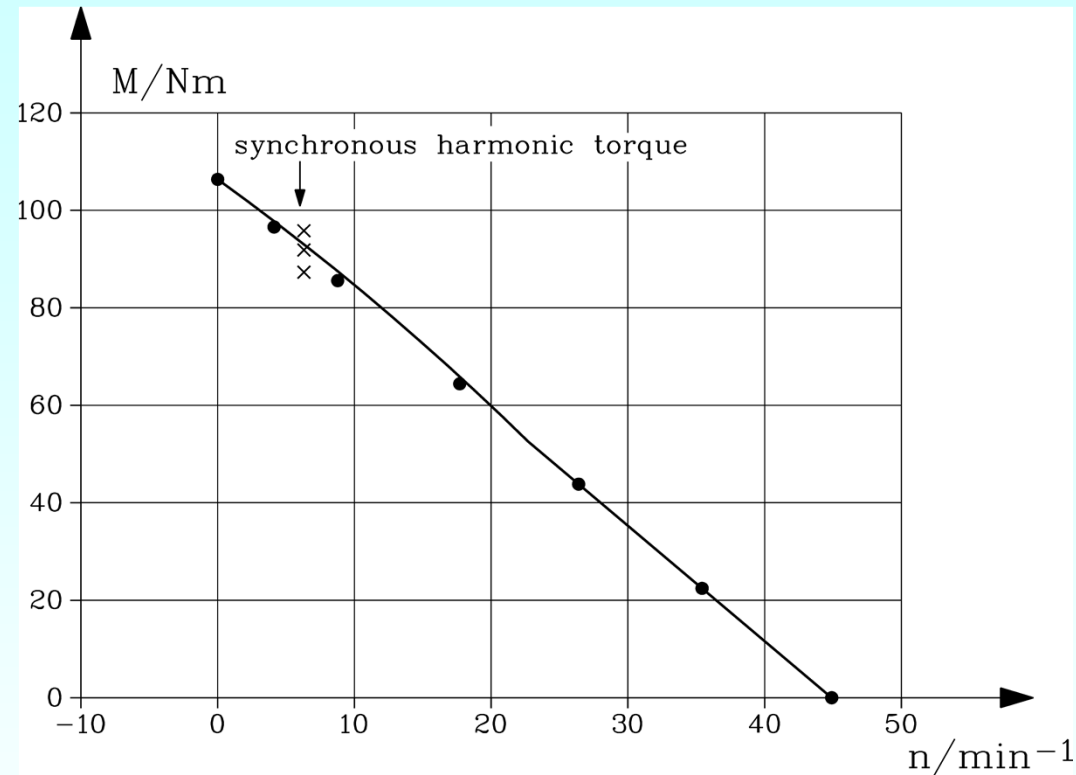
SMALL harmonic torque at inverter operation with rated current



50 Hz

550 % rated current

Big synchronous harmonic torque



1.5 Hz

100 % rated current

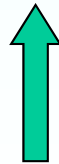
Small synchronous harmonic torque

Source:
Arkkio, A.; ICEM, 1992

Unskewed induction motors for inverter operation

- Inverter-fed motors start via frequency control with rated current, so the harmonic torques are small. **Therefore no skewing is necessary!**
- **Advantage** of unskewed induction motors:
 - Minimization of inter-bar currents = **reduction of additional losses !**
 - Maximum magnetic coupling between stator and rotor winding = Increase of main inductance, no skew leakage reactance = **total leakage flux is reduced !**
- As in unskewed induction motors there are nearly no inter-bar currents, the rotor slot number may be bigger than the stator slot number: $Q_r > Q_s!$
 - **Advantage:** At $Q_r > Q_s$ the ratio Q_r/p increases. The rotor air-gap field gets more sinusoidally distributed = the rotor harmonic leakage flux is reduced = **total leakage flux is reduced !**
- Reduction of total leakage flux = reduction of *BLONDEL*'s coefficient σ = **increase of breakdown torque M_b** according to *KLOSS*'s function!

$$M_b \approx \frac{m_s}{2} \frac{p}{\omega_s} U_s^2 \frac{1-\sigma}{\sigma X_s}$$



Example: Six-pole **unskewed** cage induction machine:
 $Q_s = 36, Q_r = 42 > 36$

